A Study of the Mechanism of the Development of Wind-wave Spectrum(Dissertation_全文)

AUTHOR(S):

Ichikawa, Hiroshi

A Study on the Mechanism of the Development of Wind-wave Spectrum

Hiroshi ICHIKAWA

主論文

A Study on the Mechanism of the Development of Wind-wave Spectrum

Part I A Model on the Turbulent Wind Field over Wind-waves in Curvilinear Co-ordinates

Part II The Energy Balance in the Wind-wave Spectrum

by

Hiroshi ICHIKAWA

Part I

A Model on the Turbulent Wind Field over Wind-waves in Curvilinear Co-ordinates

Hiroshi ICHIKAWA**

Abstract:

A new theoretical model (Model II) on the turbulent wind field over wind-waves is proposed by the use of the curvilinear orthogonal system of co-ordinates in which we can easily take into account the mean flow undulation caused by the corrugation of wavy water surface and also we can give the boundary conditions right at the wavy water surface. The numerical solutions calculated from the present linear model are in good agreement with the experimental results obtained by ICHIKAWA and IMASATO(1976). The good agreement, which was not obtained from the previous model (Model I) using the Cartesian system of co-ordinates, is attributed to the adoption of the curvilinear orthogonal system of co-ordinates.

1. Introduction

In order to understand the mechanism of the momentum and energy transfers from wind to waves, it is necessary to clarify the structure of wind field over wind-waves. ICHIKAWA and IMASATO(1976) found that the vertical change of the wave-induced fluctuations of wind velocities over wind-waves and the wave-induced Reynolds stress are different from those predicted by the Miles'(1957) quasi-laminar model. They compared

** Geophysical Institute, Faculty of Science, Kyoto University, Kitashirakawa Oiwake-cho, Sakyo-ku, Kyoto, 606 Japan

their experimental results with the numerical solutions obtained from a linear model (hereafter refered to be as Model I) on the turbulent wind field over wind-waves, and showed that the discrepancy can be attributed to the existence of the atmospheric turbulence which was neglected by MILES(1957).

However, the Model I in which the turbulent wind field is formulated in the Cartesian co-ordinates and the boundary conditions are given at the mean water surface level was not necessarily appropriate to predict the wind field over wind-waves. Actually, it could not predict the phase-differences between the wave-induced fluctuations of wind velocities and the underlying wind-waves. The critical layer, which plays an important role in the development of wind-waves, is undulated by the corrugation of wavy boundary surface and this undulating critical layer crosses the mean water surface level in many cases of wind tunnel experiment where the mean height of the undulating critical layer is lower than the wave-crests. Therefore, it is not appropriate to give the boundary conditions at the mean water surface level. It can be concluded that the discrepancy in the previous paper of ICHIKAWA and IMASATO(1976) is attributed to the facts that the boundary conditions were given at the mean water surface level assuming the infinitesimal wave and that the undulation of mean air flow was not taken into account.

In order to overcome these weak points, the adoption of the curvilinear orthogonal system of co-ordinates is the most natural way, i.e., in the curvilinear co-ordinates (ξ, η), the boundary conditions can

be given right at the wavy boundary surface and the undulating critical layer can be easily represented by an undulating line of a constant value of η. MILES(1959) and BENJAMIN(1959) have already discussed the wind field over wavy water surface using the curvilinear co-ordinates. However, neither of them took into account the existence of the atmospheric turbulence which plays an important role in the wind field over wind-waves (ICHIKAWA and IMASATO, 1976). Recently, GENT and TAYLOR(1976) numerically investigated the turbulent wind field over wavy boundary surface using the curvilinear co-ordinates. However, they neglected the existence of the viscous sublayer which will exist when the wind speed is fairly small (IMASATO, 1976).

Therefore, in this paper, another theoretical model (hereafter refered to be as Model II) on the turbulent wind field is proposed using the curvilinear co-ordinates and the numerical solutions will be compared with the previous results in the wind tunnel experiment (ICHIKAWA and IMASATO, 1976). In Model II, the existence of the viscous sublayer neglected by GENT and TAYLOR(1976) is taken into account and the influence of the underlying wind-wave field to the background atmospheric turbulence is also taken into account by introducing the parameter α representing the rate of increase of eddy viscosity due to underlying wind-wave field.

2. Theoretical Model

2.1 System of co-ordinates and govering equations

Using the curvilinear orthogonal system of co-ordinates (ξ_1, ξ_2,

ξ_3) illustrated in Fig. 1, we consider the turbulent wind field in a frame of reference travelling with the phase velocity $\underline{C}$ of an underlying component wave in positive x_1-direction. The Cartesian system of co-ordinates (x_1, x_2, x_3), which is also illustrated in Fig. 1, is expressed in the curvilinear system of co-ordinates as follows,

Fig. 1

$$\begin{cases} x_1 = \xi_1 - a \exp(-k\xi_3) \sin(k\xi_1), \\ x_2 = \xi_2, \\ x_3 = \xi_3 + a \exp(-k\xi_3) \cos(k\xi_1). \end{cases}$$

where $\underline{a}$ is the wave-amplitude and $\underline{k}$ the wave-number of the component wave. The wavy water surface, represented in the curvilinear co-ordinates as $\xi_3 = 0$, is expressed in the Cartesian co-ordinates as follows,

$$x_3 = a \cos(k\xi_1) \qquad (2.1)$$

which equals $a \cos(kx_1)$ to the order of $\underline{ak}$.

It is assumed in this paper that $(\underline{ak})^2$ is negligibly small, the wind field is homogeneous in the x_2-direction and that the mean horizontal velocity $U(x_3) - C$ in the reference frame has only the component parallel to the x_1-axis.

The ξ_n-component of wind velocity u_n in the turbulent wind field over wavy boundary surface in the reference frame is decomposed into the mean component $\bar{u}_n$, the wave-induced periodic component $\tilde{u}_n$ and the random background turbulence u_n'; i.e.,

$$u_n(\xi_1, \xi_3, t) = \bar{u}_n(\xi_3) + \tilde{u}_n(\xi_1, \xi_3) + u_n'(\xi_1, \xi_3, t)$$

where t is the time. The time average, denoted by operator $\langle\ \rangle$, of the wind velocity can be represented by

$$\langle u_n \rangle = \bar{u}_n(\xi_3) + \tilde{u}_n(\xi_1, \xi_3).$$

The mean wind velocity $\bar{u}_n$ is assumed to be expressed in the reference frame as follows,

$$\bar{u}_n(\xi_3) = (U(x_3) - C, 0, 0), \qquad (2.2)$$

where $U(x_3) - C$ is the mean horizontal wind velocity at the height $x_3 = \xi_3$.

Owing to this treatment, the mean wind velocity in the region between a wave-crest and a wave-trough can be derived although it can not be treated in the Cartesian co-ordinates, and the mean flow undulation caused by the corrugation of wavy boundary surface can be easily introduced in the analysis as a mean flow parallel to the ξ_1-axis.

The time average of the vorticity equation on the turbulent wind field over wavy boundary can be expressed in vector form as follows,

$$\langle \mathrm{rot.}(\mathrm{rot.}\bar{u} \times \bar{u} + \mathrm{rot.}\tilde{u} \times \bar{u} + \mathrm{rot.}\bar{u} \times \tilde{u}) \rangle$$

$$= -\nu_a \langle \mathrm{rot.rot.rot.}u \rangle + \Pi + W, \qquad (2.3)$$

where ν_a is the kinematic molecular viscosity of air, Π the contribution from atmospheric turbulence neglected by BENJAMIN(1959) and W the contribution from wave-induced velocity fluctuations. Π

and W are denoted by Eqs.(2.4) and (2.5), respectively.

$$T = \langle -\mathrm{rot.}(\mathrm{rot.}u' \times u') \rangle, \qquad (2.4)$$

$$W = \langle -\mathrm{rot.}(\mathrm{rot.}\tilde{u} \times \tilde{u}) \rangle. \qquad (2.5)$$

In order to obtain the solution of Eq.(2.3) on $\tilde{u}$, the mean wind velocity, the contribution from atmospheric turbulence and the boundary conditions must be determined.

2.2 Stream function

Before describing the assumptions adopted in this paper, we define here the stream function as follows,

$$\langle u_1 \rangle = J^{\frac{1}{2}} \frac{\partial}{\partial \xi_3} \psi \qquad \text{and} \qquad \langle u_3 \rangle = -J^{\frac{1}{2}} \frac{\partial}{\partial \xi_1} \psi$$

where J is the Jacobian of the transformation. The stream function $\psi(\xi_1, \xi_3)$ is represented as follows,

$$\psi(\xi_1, \xi_3) = \bar{\psi}(\xi_3) + \tilde{\psi}(\xi_1, \xi_3)$$

where $\bar{\psi}(\xi_3)$ is the undisturbed part defined by

$$\bar{\psi}(\xi_3) = \int_0^{\xi_3} \bar{u}_1(\xi_3)\, d\xi_3$$

and $\tilde{\psi}$ the wave-induced periodic part. $\tilde{\psi}$ is assumed to be represented by

$$\tilde{\psi}(\xi_1, \xi_3) = ak\, \mathcal{R}_e\{\hat{\psi}(\xi_3) \exp(jk\xi_1)\}$$

where $\mathcal{R}_e$ indicates the real part of a complex variable, $\hat{\psi}$ the complex

amplitude of $\tilde{\varphi}$ and $j = \sqrt{-1}$.

Hereafter all variables and co-ordinates will be expressed in non-dimensional form, taking $\underline{k}^{-1}$ and $\underline{C}$ as the scales of the length and the velocity, respectively.

2.3 Turbulent Reynolds stresses

The turbulent Reynolds stress r_{nm} is denoted by

$$r_{nm} = \langle -u_n' u_m' \rangle$$

$$= \bar{r}_{nm}(\xi_3) + \tilde{r}_{nm}(\xi_1, \xi_3) \qquad (2.6)$$

where $\bar{r}_{nm}$ is the mean part and $\tilde{r}_{nm}$ the wave-induced periodic part which is assumed to be represented by

$$\tilde{r}_{nm}(\xi_1, \xi_3) = a\,\mathcal{R}e\{\hat{r}_{nm}(\xi_3)\exp(j\xi_1)\}$$

where $\hat{r}_{nm}$ is the complex amplitude of $\tilde{r}_{nm}$.

Using the equation of continuity about the turbulent fluctuations of wind velocity, the ξ_2-component T_2 of Π, correct to the order of $\underline{a}$, can be represented as follows,

$$T_2 = \bar{r}_{13}'' + a\,\mathcal{R}e\Big[\Big\{\hat{r}_{13}'' + \hat{r}_{13} + j(\hat{r}_{11}' - \hat{r}_{33}')$$

$$+ 2\exp(-\xi_3)\left(\tfrac{1}{2}j(\bar{r}_{33}' - \bar{r}_{11}') - j(\bar{r}_{33} - \bar{r}_{11})\right.$$

$$\left.+ (\bar{r}_{13}'' + \bar{r}_{13}' - 2\bar{r}_{13})\right)\Big\}\exp(j\xi_1)\Big]$$

where prime denotes the differentiation on ξ_3. Therefore, the turbulent Reynolds stress r_{nm} must be determined in order to solve Eq.(2.3).

The mean tangential turbulent Reynolds stress $\bar{r}_{13}$ is obtained from overall average of the equation of motion and represented by

$$\bar{r}_{13}(\xi_3) = u_*^2 - \nu_a \bar{u}_1'(\xi_3), \qquad (2.7)$$

where $\bar{u}_1'$ is the vertical shear of mean wind velocity and u_* the friction velocity of air. On the other hand, we have no information on the vertical changes of the mean normal turbulent Reynolds stresses over wind-waves. From the experimental results on the pipe flow (HINZE, 1959, Figs.7-34 and 7-38), they are assumed in this paper as follows,

$$\bar{r}_{11}(\xi_3) = -5.8\, \bar{r}_{13}(\xi_3), \qquad (2.8)$$

$$\bar{r}_{33}(\xi_3) = -0.6\, \bar{r}_{13}(\xi_3). \qquad (2.9)$$

The wave-induced variations of turbulent Reynolds stresses $\tilde{r}_{nm}$ are assumed to have the same form as in Model I and Yefimov's(1970) model, i.e.,

$$\tilde{r}_{11} = \tilde{r}_{33}, \qquad (2.10)$$

$$\tilde{r}_{13} = 2\, \nu_e \tilde{e}_{13}$$

$$= 2\, \nu_e\, a\, \mathcal{R}e\{\hat{e}_{13}(\xi_3) \exp(j\xi_1)\}, \qquad (2.11)$$

where ν_e is the eddy viscosity and $\hat{e}_{13}$ the complex amplitude of the wave-induced variation $\tilde{e}_{13}$ of tangential rate-of-strain. $\hat{e}_{13}$ is expressed by Eq.(2.12) in the curvilinear co-ordinates.

$$\hat{e}_{13}(\xi_3) = \tfrac{1}{2}\{\hat{\psi}''(\xi_3) + \hat{\psi}(\xi_3) + 2\exp(-\xi_3)(\bar{u}_1' - \bar{u}_1)\} \qquad (2.12)$$

Although the eddy viscosity ν_e was assumed to be constant with respect to x_3 in Model I, it is assumed in this paper to be several times greater than the eddy viscosity ν_s associated with the vertical shear of mean wind velocity as follows,

$$\nu_e(\xi_3) = \alpha\ \nu_s(\xi_3), \qquad (2.13)$$

where α is a non-dimensional parameter with a positive constant value and ν_s satisfies the following equation,

$$\bar{r}_{13}(\xi_3) = 2\ \nu_s(\xi_3)\ \bar{e}_{13}(\xi_3)$$
$$= \nu_s(\xi_3)\ \bar{u}_1'(\xi_3)$$

where $\bar{e}_{13}$ is the mean tangential rate-of-strain. It must be noticed that Eq.(2.11) corresponds to the following equation in the Cartesian co-ordinates,

$$\tilde{r}_{13} = \nu_e\ (\frac{\partial}{\partial x_1}\tilde{v}_3 + \frac{\partial}{\partial x_3}\tilde{v}_1),$$

where $\tilde{v}_n$ is the wave-induced fluctuation of x_n-component of wind velocity. REYNOLDS and HUSSAIN(1972) and DAVIS(1972) proposed the relation of Eq.(2.13) with $\alpha = 1$, which means that the eddy viscosity ν_e is always equal to the eddy viscosity associated with the vertical shear of mean wind velocity. However, the eddy viscosity ν_e in Eq.(2.11) is a coefficient which relates $\tilde{r}_{13}$ with $\tilde{e}_{13}$, and therefore, it is assumed here that the value of α is not always unity. The parameter α is considered to represent the influence of the wind-wave field to the background turbulence. The value of α can not be determined from

the measurement and we inevitably obtain the numerical solutions for several values of α from 0.5 to 20.

2.4 Mean wind profile

It is well known that the vertical profile of the mean horizontal wind velocity $U(x_3)$ in the turbulent boundary layer over wind-waves is logarithmic with respect to x_3. On the other hand, in the close vicinity of the wavy water surface, it can not be measured directly and it is assumed, as was proposed by DAVIS(1972), to be linear with respect to x_3 in the layer (named as "linear sublayer" in this paper) of which thickness z_1 equals $z_0 \exp(\Delta U)$, where ΔU is the thickness parameter of "linear sublayer".

On the other hand, the mean wind velocity $\bar{u}_1(\xi_3)$ parallel to ξ_1-axis has not been clarified yet and it is assumed in this paper to be represented by Eq.(2.2). Therefore, from the vertical profile of the mean horizontal wind velocity described above, $\bar{u}_1(\xi_3)$ is represented as follows,

$$\bar{u}_1(\xi_3) = U(\xi_3) - 1$$

$$= \begin{cases} \frac{u_*}{\kappa} \ln(\xi_3/z_0) - 1, & \xi_3 \geqq z_1 \\ \frac{u_*}{\kappa} G(\Delta U)\, \xi_3/z_0 - 1, & \xi_3 < z_1 \end{cases} \qquad (2.14)$$

where u_*, z_0 and κ are the friction velocity of air, the roughness height and the Kármán constant, respectively, and $G(\Delta U) \equiv \Delta U \exp(-\Delta U)$.

As the eddy viscosity ν_e defined by Eq.(2.13) must be zero or positive in the "linear sublayer", the value of ΔU must satify the

following relation,

$$\propto (\kappa u_* z_0 / G(\Delta U) - \nu_a) \gtreqless 0 \qquad (2.15)$$

Therefore, the value of ΔU must be greater than or equal to ΔU_m which satisfies the sign of equality in the relation (2.15) when the parameter $D = \kappa u_* z_0 / \nu_a$ is smaller than $G(1) = \exp(-1)$ because the function $G(\Delta U)$ has the maximum value at $\Delta U = 1$. The "linear sublayer" for $\Delta U = \Delta U_m$ is coincident with the viscous sublayer and in that sublayer the eddy viscosity ν_e vanishes. On the other hand, the value of ΔU can be arbitrarily positive when the parameter D is greater than $G(1)$. In any case, the value of ΔU can not be fixed from the measurements, and we inevitably obtain the numerical solutions for several values of ΔU from unity or ΔU_m to ten.

2.5 Boundary conditions and numerical method

Now, let's consider the boundary conditions, correct to the order of a, to be satisfied by the velocity components right at the wavy water surface $\xi_3 = 0$. The normal component $\langle u_3(0) \rangle$ must be zero since the wave is stationary in the present frame of reference, i.e.,

$$\hat{\eta}(0) = 0 \qquad (2.16)$$

The tangential component $\langle u_1(0) \rangle$ must satisfy the condition of non-slipping relative to the water particle right at the wavy surface. The tangential velocity u_c of the water particle right at the wavy water surface has not been well known yet. Therefore, it is assumed in this

paper that u_c equals the horizontal component of the orbital velocity of wave at $x_3 = 0$. Owing to this assumption, it is derived as follows,

$$\hat{\psi}'(0) = 1 - \bar{u}_1(0) \qquad (2.17)$$

The wave-induced periodic components of wind velocity at $\xi_3 = H$, the height sufficiently far from the wavy surface, must be vanished and this requires that

$$\hat{\psi}(H) = 0, \qquad (2.18)$$

$$\hat{\psi}'(H) = \bar{u}_1(H) \exp(-H) \qquad (2.19)$$

From the assumptions described above on the turbulent Reynolds stress, the wave-induced periodic part of the ξ_2-component of the vorticity equation (2.3), which is correct to the order of $\underline{a}$, can be derived as follows,

$$\begin{aligned} &\bar{u}_1(\hat{\psi}'' - \hat{\psi}) - \hat{\psi}\bar{u}_1'' = -j\nu_a(\hat{\psi}'''' - 2\hat{\psi}'' + \hat{\psi}) \\ &- j\nu_e(\hat{\psi}'''' + 2\hat{\psi}'' + \hat{\psi}) - 2j\nu_e'(\hat{\psi}''' + \hat{\psi}') \\ &- j\nu_e''(\hat{\psi}'' + \hat{\psi}) + A \end{aligned} \qquad (2.20)$$

where

$$\begin{aligned} A = &\left\{(\bar{r}_{33}' - \bar{r}_{11}') - 2(\bar{r}_{33} - \bar{r}_{11}) - 2j(\bar{r}_{13}' - 2\bar{r}_{13})\right\}\exp(-\xi_3) \\ &- 2\left[\bar{u}_1'\bar{u}_1 + j\left\{\nu_a(\bar{u}_1''' - 2\bar{u}_1'') + \nu_e(\bar{u}_1''' - 3\bar{u}_1'' + 4\bar{u}_1' - 2\bar{u}_1)\right.\right. \\ &\left.\left. + 2\nu_e'(\bar{u}_1'' - 2\bar{u}_1' + \bar{u}_1) + \nu_e''(\bar{u}_1' - \bar{u}_1)\right\}\right]\exp(-\xi_3) \end{aligned} \qquad (2.21)$$

and $\overline{W}$ in Eq.(2.3) is neglected because the magnitude of the wave-induced Reynolds stress is the order of $\underline{a}^2$. It is recognized that the first and the second terms in the right-hand side of Eq.(2.21) originate from our adoption of the curvilinear co-ordinates and the existence of the mean flow undulation caused by the corrugation of the wavy boundary, respectively, by comparing Eq.(2.20) with the vorticity equation formulated in the Cartesian co-ordinates by the use of the stream function ϕ_1 which is defined as follows,

$$\phi_1(x_1,x_3) = \bar{\psi}(x_3) - a\bar{u}_1(x_3)\exp(-x_3)\cos(x_1) + a\,\mathcal{R}e\{\hat{\phi}_1(x_3)\exp(jx_1)\} \qquad (2.22)$$

where $\bar{\phi}$ is the undisturbed part, the second term is the contribution from mean flow undulation caused by the corrugation of wavy boundary, which is correct to the order of $\underline{a}$, and $\hat{\phi}_1$ is the complex amplitude of the wave-induced periodic part.

The finite differential equation derived from Eq.(2.20) is integrated numerically with the boundary conditions given at $\xi_3 = 0$ and $\xi_3 = H$. The finite difference length $\Delta\xi_3$ and the upper limit H of the integration are chosen to be 0.001 and 4.0, respectively, because the numerical solution obtained for $\Delta\xi_3 = 0.0005$ and H = 6.0 is nearly equal to that obtained for $\Delta\xi_3 = 0.001$ and H = 4.0 although it is not illustrated in any figure.

3. Results and discussion

3.1 Numerical results

The numerical solutions and the experimental results (ICHIKAWA and IMASATO, 1976) are compared in quantities σ_u^2, σ_w^2, θ_u, θ_w and τ, which are the non-dimensional powers of the wave-induced fluctuations of horizontal and vertical wind velocities, the phase-differences of the wave-induced fluctuations of horizontal and vertical wind velocities from the underlying component wave, and the non-dimensional wave-induced Reynolds stress, respectively. It must be noticed that these quantities in the following discussion are the spectral components with the frequency f_p of the wave spectral peak. They are expressed as follows,

$$\sigma_u^2 = \tfrac{1}{2}|\hat{\phi}'|^2, \qquad \sigma_w^2 = \tfrac{1}{2}|\hat{\phi}|^2,$$

$$\theta_u = \tan^{-1}(-\hat{\phi}'_i/\hat{\phi}_r),$$

$$\theta_w = \tan^{-1}(\hat{\phi}_r/\hat{\phi}_i),$$

$$\tau = \tfrac{1}{2}(\hat{\phi}'_i\hat{\phi}_r - \hat{\phi}'_r\hat{\phi}_i), \qquad (3.1)\sim(3.5)$$

where suffixes r and i represent the real and imaginary parts, respectively, and $\hat{\phi}$ is the complex amplitude of the wave-induced periodic part of the stream function defined in the Cartesian co-ordinates. Owing to the relations between the Cartesian co-ordinates and the curvilinear co-ordinates, $\hat{\phi}$ can be related with $\hat{\psi}$, which satisfies Eq.(2.20) at $\zeta_3 = x_3$, as represented by the following equations.

$$\hat{\phi}(x_3) = \hat{\psi}(x_3) - \exp(-x_3)(U(x_3) - 1) \qquad (3.6)$$

$$\hat{\phi}'(x_3) = \hat{\mathcal{F}}'(x_3) - \exp(-x_3)(U'(x_3) - U(x_3) + 1) \qquad (3.7)$$

Each second term in the right-hand side of Eqs.(3.6) and (3.7) represents the contribution from mean flow undulation caused by the corrugation of wavy boundary surface to the wave-induced fluctuations of vertical and horizontal wind velocities, respectively.

In order to solve Eq.(2.20) numerically, the values of u_*, z_0, ΔU and α are necessary to be given. u_* and z_0 are the known values from the wind tunnel experiment, but the parameters ΔU and α must be suitably determined in order that the numerical solutions agree with the experimental results.

Figs. 2, 3 and 4 show the measured and calculated vertical profiles of σ_u^2, σ_w^2, θ_u, θ_w and τ in the experimental cases of Run-I, II and III (ICHIKAWA and IMASATO, 1976), respectively. The numerical solutions in these figures are obtained for some values of α from two to ten, from Model II proposed in this paper. The conditions of the vertical profile of mean wind velocity and the wind-wave field in the experimental cases of Run-I, II and III are tabulated in Table 1. The values of ΔU used in the calculation of the numerical solutions shown in Figs. 2 and 3 are 7.49 and 2.75, respectively, which correspond to the minimum value ΔU_m in each experimental case. On the other hand, the parameter $D = \kappa u_* z_0 / \nu_a$ is greater than G(1) and the value of ΔU_m can not be determined in the experimental case of Run-III. Since the parameter ΔU determines the "linear sublayer" thickness z_1 and the mean wind velocity only in the "linear sublayer", the influence of ΔU on the calculated vertical profiles in the region much higher

than z_1 is fairly small as long as z_1 is much smaller than unity although it is not illustrated in any figure. The value of ΔU in Run-III is chosen so that z_1 is much smaller than unity. The numerical solutions obtained for $\Delta U = 3.0$ are shown in Fig. 4 as an example.

It is known from Figs. 2, 3 and 4 that the vertical profiles obtained from our present Model II with a suitable value of α have good agreement with measured ones, especially the vertical profiles of θ_u and θ_w which were not well predicted by Model I. The suitable values of α in the cases of Run-II and III are found to be in the range from two to ten. But it is apparent that the suitable value of α to explain the measured vertical change of σ_u^2 in the case of Run-I is in the range from five to ten. This result suggests that the parameter α may depend on the underlying wind-wave field and the friction velocity of air. The precise discussion about the parameter α will be made in the following paper.

3.2 Turbulent Reynolds stresses

We have no information on the mean normal turbulent Reynolds stresses and the wave-induced variation of turbulent Reynolds stresses and they are assumed as described in section 2.3. REYNOLDS and HUSSAIN (1972) proposed another model in which $\tilde{r}_{11}$ and $\tilde{r}_{33}$ are related to the wave-induced variation of normal rate-of-strain, respectively. They are represented in the curvilinear co-ordinates as follows,

$$\tilde{r}_{11}(\xi_3) = 2\nu_e \mathcal{R}e\left[\{-j\hat{\psi}' + \exp(-\xi_3)\bar{u}_1\}\exp(j\xi_1)\right], \quad (3.8)$$

$$\tilde{r}_{33}(\xi_3) = 2\nu_e \mathcal{R}e\left[\{-j\hat{\psi}' - \exp(-\xi_3)\bar{u}_1\}\exp(j\xi_1)\right]. \quad (3.9)$$

The numerical solutions obtained from Model IIa in which $\tilde{r}_{11}$ and $\tilde{r}_{33}$ are given by Eqs.(3.8) and (3.9) instead of Eq.(2.10), respectively, are nearly equal to those obtained from Model II although they are not illustrated in any figure.

It must be noticed that the representation of the mean normal turbulent Reynolds stresses is not crucial. The numerical solution obtained from another model in which the mean normal turbulent Reynolds stresses are equal to each other, are nearly equal to those obtained from Model II although they are not shown in any figure.

3.3 Undulation of mean flow

Model II differs from our previous Model I not only in the co-ordinates system but also in introducing the mean flow undulation and in the assumptions on the eddy viscosity and on the vertical profile of mean wind velocity in the close vicinity of wavy surface. In order to examine the influence of the difference between the assumptions adopted in Model II on the eddy viscosity and on the vertical profile of mean wind velocity and those adopted in Model I, another numerical calculation (named as Model IIb) was performed in the curvilinear co-ordinates under the same assumptions as is adopted in Model I; i.e., the eddy viscosity is constant with respect to ξ_3 and the value of ΔU is zero.

Figs. 5a and 5b show the measured and calculated vertical profiles of θ_u and θ_w in the experimental case of Run-II. The calculated vertical profiles in these figures are obtained from Model I and IIb

with the same value ($1.5 \times 10^3 cm^2 s^{-1}$) of the eddy viscosity. From the comparison between the solutions for Model IIb and the solutions in Fig. 3 for Model II, it can be said that the numerical results obtained from Model IIb and Model II are nearly equal to each other. Further, it is seen in Figs. 5a and 5b that the numerical results obtained from Model IIb are largely different from those obtained from Model I in spite of the fact that the assumptions on the eddy viscosity and on the value of ΔU adopted in Model IIb are equal to those adopted in Model I. Therefore, the good agreement between the experimental and the numerical results shown in Figs. 2, 3 and 4 can be attributed to the adoption of curvilinear co-ordinates and to the introduction of undulation of mean flow. The origin of the large difference between the numerical results obtained from Model I and those obtained from Model IIb is described as follows.

The undisturbed part $\bar{\mathcal{F}}(\xi_3)$ of the stream function defined in the curvilinear co-ordinates, which originally represents the mean flow undulation caused by the corrugation of wavy boundary, is expressed by the Taylor series expansion in the Cartesian co-ordinates as follows,

$$\bar{\mathcal{F}}(\xi_3) = \phi_2(x_1,x_3) + \tfrac{1}{2}\bar{u}_1'(x_3)\{-a\exp(-x_3)\cos(x_1)\}^2 + \tfrac{1}{6}\bar{u}_1''(x_3)\{-a\exp(-x_3)\cos(x_1)\}^3 + \ldots \quad (3.10)$$

where

$$\phi_2(x_1,x_3) = \bar{\phi}(x_3) - a\,\bar{u}_1(x_3)\exp(-x_3)\cos(x_1)$$

It must be noticed that only the term ϕ_2 can be used in a linear theory in the Cartesian co-ordinates to represent the undulation of

mean flow as is seen in Eq.(2.22). However, the mean flow undulation, which must be introduced in the analysis, can not be completely represented by ϕ_2 alone because $\bar{u}_1(x_3)$ vanishes at the critical height $x_3 = z_c$ and $\phi_2(x_1, x_3)$ has a constant value of $\bar{\phi}(z_c)$ at $x_3 = z_c$, i.e., the stream line corresponding to $\phi_2(x_1, x_3) = \bar{\phi}(z_c)$ is parallel to x_1-axis at $x_3 = z_c$. Further more, the stream line corresponding to $\phi_2 = \bar{\phi}(z_c)$ crosses the wavy boundary surface in many cases of wind tunnel experiment where the critical height is lower than wave-crests. In order to represent the undulation of mean flow, at least the second term in the right-hand side of Eq.(3.10) must be introduced in the analysis because the value of this term changes with respect to x_1 at $x_3 = z_c$. The higher order terms than the order of $\underline{a}^2$ in the right-hand side of Eq.(3.10) are originally included in the linear model Model IIb in the curvilinear co-ordinates by the use of $\bar{\psi}(\zeta_3)$. On the other hand, these higher order terms can not be treated in the linear model Model Ia in which the undulation of mean flow is taken into account only to the order of $\underline{a}$ in the Cartesian co-ordinates by the use of the stream function ϕ_1 defined by Eq.(2.22). It can be easily derived that the numerical result obtained from Model Ia coincides with the numerical solution of Model I. Therefore, the large difference between the numerical results obtained from Model I and Model IIb originates from the higher order terms than the order of $\underline{a}^2$ in the right-hand side of Eq.(3.10). It can be concluded that the good agreement between the experimental and numerical results shown in Figs. 2, 3 and 4 is attributed to the fact that the undulation of

mean flow is well represented in the linear model Model II by the use of the curvilinear co-ordinates. This result suggests that the momentum and energy transfers from turbulent wind to waves also must be estimated in the curvilinear co-ordinates when the mean height of undulating critical layer is lower than wave-crests.

It must be emphasized at last that the direct measurement of the background atmospheric turbulence in the mysterious region between the crests and troughs of wind-waves is greatly important.

Acknowlegements

The author wishes to express his thanks to Prof. H. KUNISHI of Kyoto University for his discussion and encouragement. He also expresses his gratitude to Dr. N. IMASATO of Kyoto University for his gracious discussion throughout this study. Thanks must be extended to Mrs. A. OOTANI for typing the manuscript. The numerical calculations in this article were carried out on FACOM 230-75 and FACOM M 190 in the Data Processing Center of Kyoto University.

References

BENJAMIN, T.B. (1959): Shearing flow over a wavy boundary. J. Fluid Mech., 6, 161-205.

DAVIS, R.E. (1972): On the prediction of the turbulent flow over a wavy boundary. J. Fluid Mech., 52, 287-306.

GENT, P.R. and P.A. TAYLOR (1976): A numerical model of the air flow above water waves. J. Fluid Mech., 77, 105-128.

HINZE, J.O. (1959): Turbulence. Mcgraw-Hill Book Co. Inc., New York, 586 pp.

ICHIKAWA, H. and N. IMASATO (1976): The wind field over wind-waves. J. Oceanogr. Soc. Japan, 32, 271-283.

IMASATO, N. (1976): The mechanism of the development of wind-wave spectra. J. Oceanogr. Soc. Japan, 32, 253-266.

MILES, J.W. (1957): On the generation of surface waves by shear flows. J. Fluid Mech., 3, 185-204.

MILES, J.W. (1959): On the generation of surface waves by shear flows. Part 2. J. Fluid Mech., 6, 568-582.

REYNOLDS, W.C. and A.K.M.F. HUSSAIN (1972): The mechanics of an organized wave in turbulent shear flow. Part 3. Theoretical models and comparisons with experiments. J. Fluid Mech., 54, 263-288.

YEFIMOV, V.V. (1970): On the structure of the wind velocity field in the atmospheric near-water layer and the transfer of wind energy to sea waves. Izv. Atmos. Oceanic Physics, 6, 1043-1053.

風波上の乱れた風の場に関する曲線座標系でのモデル

市川　洋**

要旨：曲線直交座標系を用いて風波の上の乱れた風の場についての新たな理論モデル（Model Ⅱ）を提案する。この座標系の採用によって、波面の凹凸の乱れた風の場への影響を考慮に入れることができるとともに、波面そのもので境界条件を与えることができる。この線形モデルから計算される数値解はICHIKAWA and IMASATO（1976）によって得られた実験結果と良く一致した。デカルト座標系を用いた以前のモデル（Model Ⅰ）では得られなかった実験との良い一致はModel Ⅱで曲線直交座標系を採用したことによることが示される。

** 京都大学理学部地球物理学教室，〒606 京都市左京区北白川追分町

Table 1. The conditions of the vertical profile of mean wind velocity and the wind-wave field.

Fig. 1. Curvilinear orthogonal system of co-ordinates (ξ_1, ξ_2, ξ_3) and Cartesian system of co-ordinates (x_1, x_2, x_3).

Fig. 2. Vertical profiled of σ_u^2, σ_w^2, θ_u, θ_w and τ obtained from Model II corresponding to the experimental case of Run-I and those of the observed values (mark ●). The variable range of θ_u, θ_w and τ under the 95 % confidence limit is shown by the line through the closed circle. x_3 is the height non-dimensionalized by the wave-number. The value of α is in the range from 2.0 to 10.0.

Fig. 3. Vertical profiles of σ_u^2, σ_w^2, θ_u, θ_w and τ calculated from Model II in the experimental case of Run-II and those of the observed values.

Fig. 4. Vertical profiles of σ_u^2, σ_w^2, θ_u, θ_w and τ calculated from Model II in the experimental case of Run-III and those of the observed values.

Fig. 5a. Vertical profiles of θ_u calculated from Model I and Model IIb in the experimental case of Run-II and those of the observed value. The variable range of θ_u under the 95 % confidence limit is shown by the line through the closed circle. The value of ν_e is 1.5×10^3 $cm^2 s^{-1}$.

Fig. 5b. Vertical profiles of θ_w calculated from Model I and Model IIb in the experimental case of Run-II and those of the observed value.

		Run-I	Run-II	Run-III
u_*	(cm s^{-1})	9.39	23.0	43.3
z_0	(cm)	0.000167	0.00286	0.0209
f_p	(Hz)	3.60	2.30	1.80
k	(cm^{-1})	0.512	0.212	0.130
mean amplitude	(cm)	0.132	0.840	1.74
u_* / C		0.212	0.338	0.499

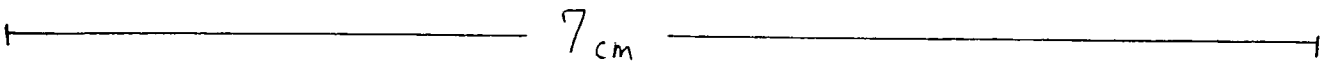

Table 1.

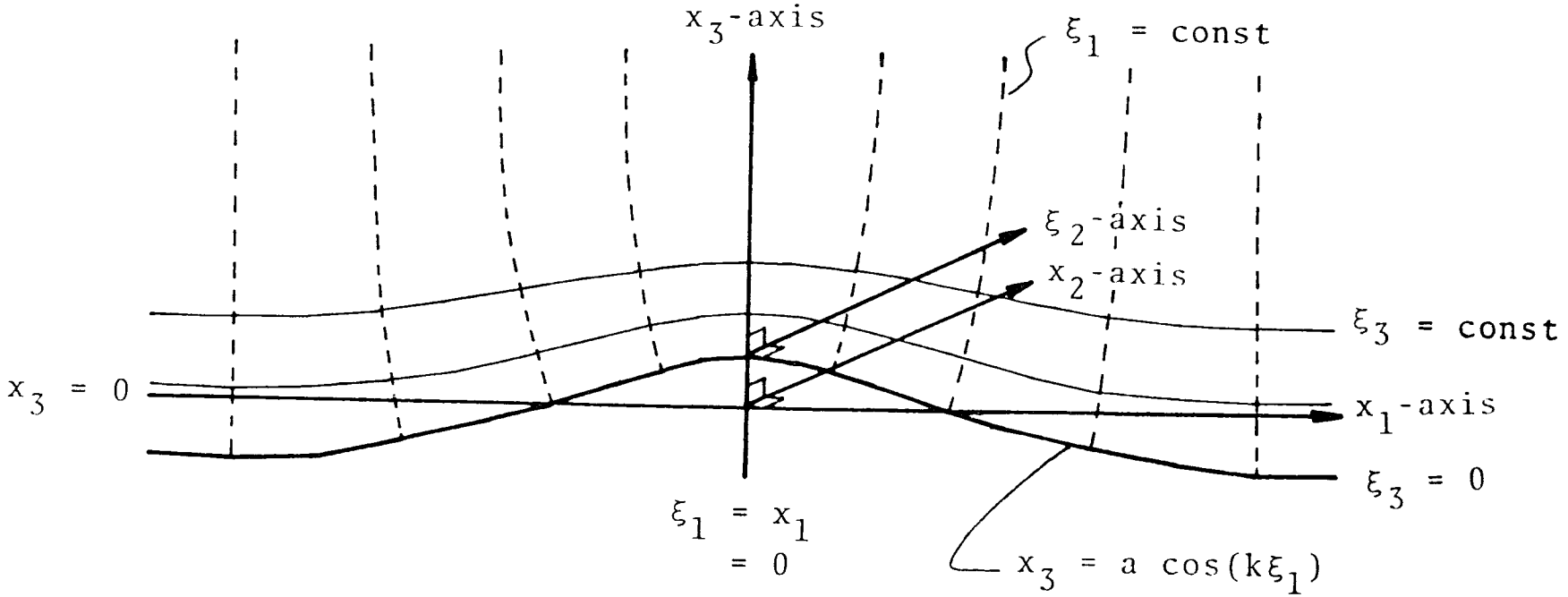
x_3-axis
ξ_1 = const
ξ_2-axis
x_2-axis
ξ_3 = const
x_3 = 0
x_1-axis
ξ_3 = 0
$\xi_1 = x_1 = 0$
$x_3 = a \cos(k\xi_1)$

17 cm

Fig. 1.

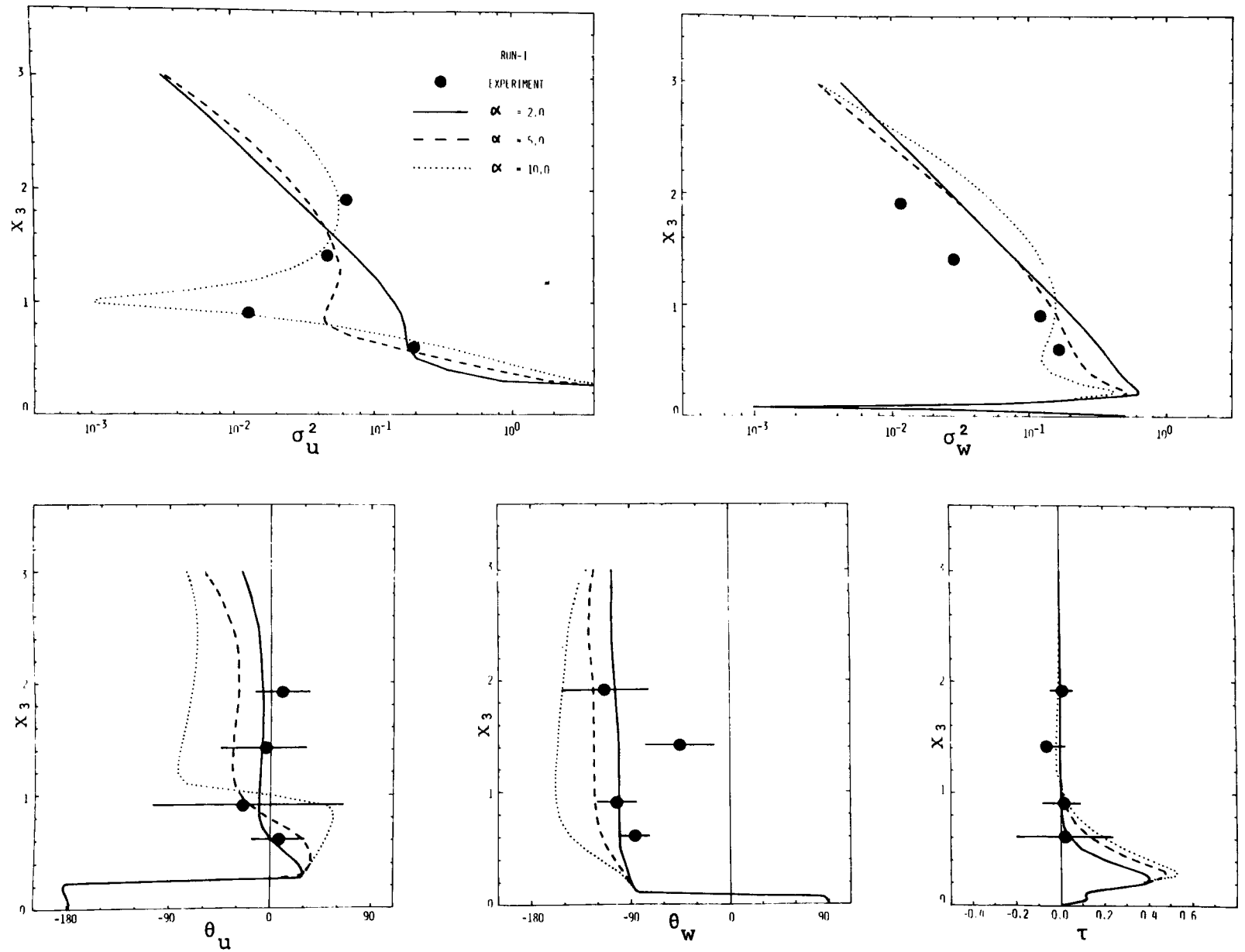
RUN-1
EXPERIMENT
α = 2.0
α = 5.0
α = 10.0
x_3
σ_u^2
σ_w^2
θ_u
θ_w
τ

14 cm

Fig. 2.

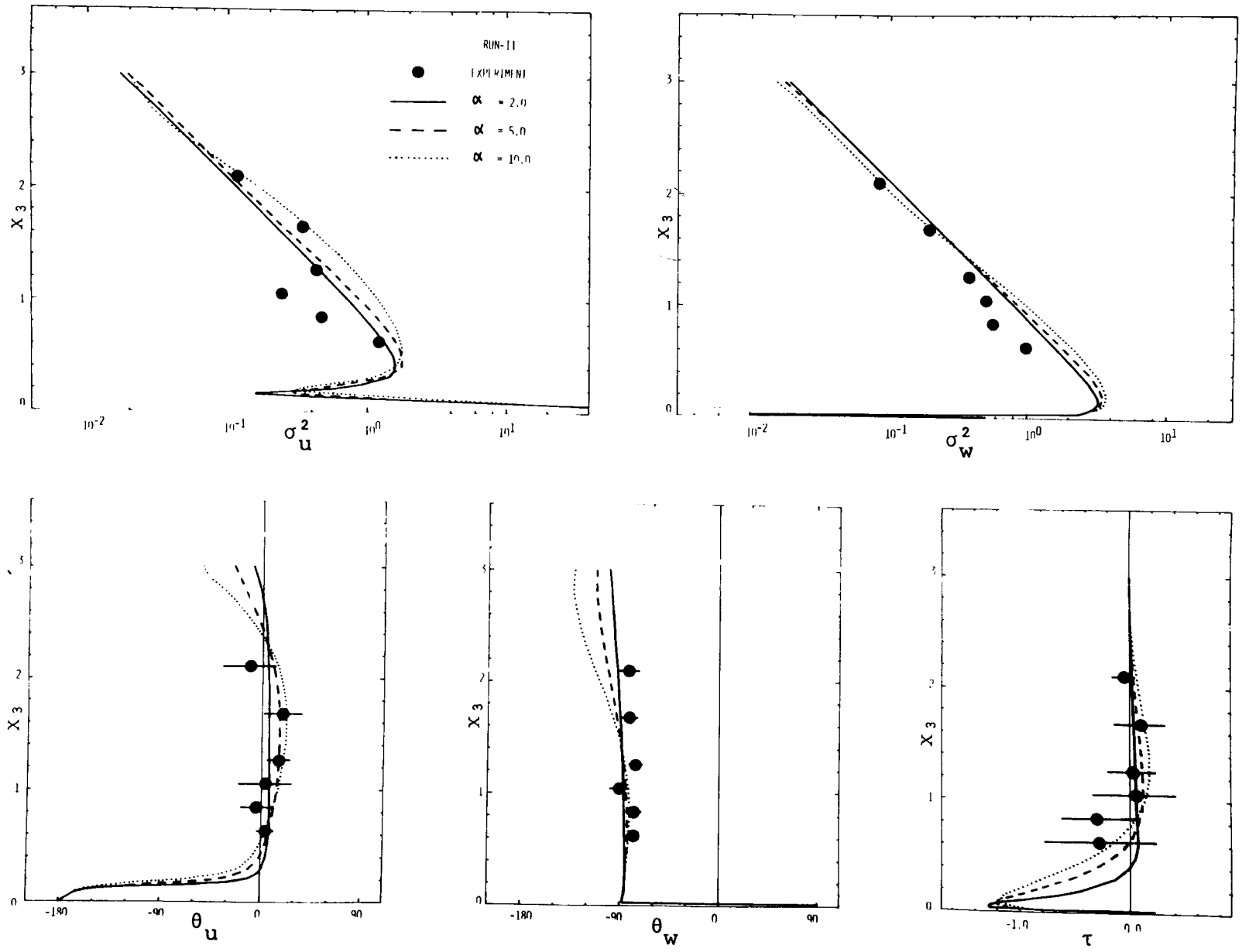
RUN-11
EXPERIMENT
α = 2.0
α = 5.0
α = 10.0
X_3
σ_u^2
σ_w^2
θ_u
θ_w
τ

14 cm

Fig. 3.

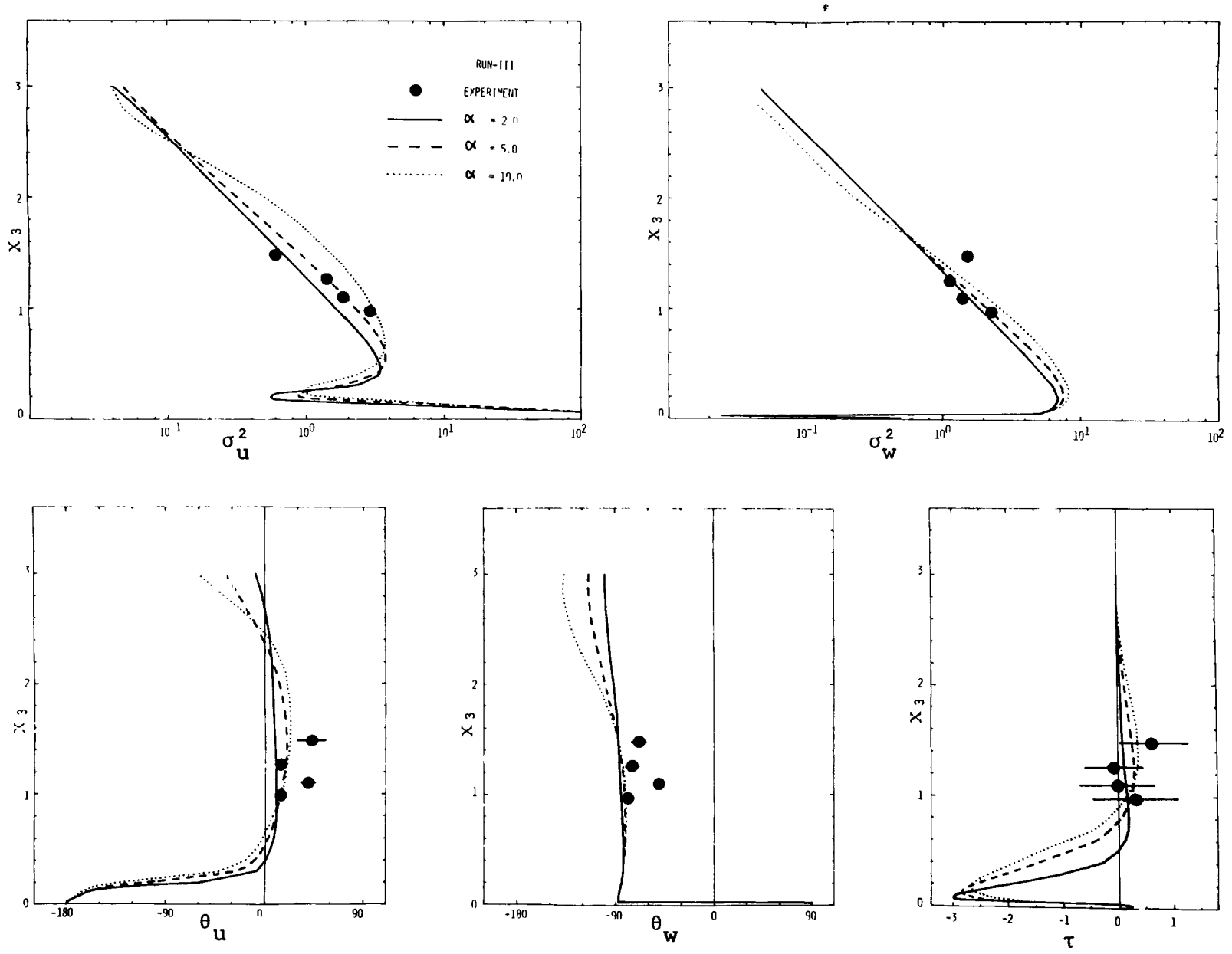

14 cm

Fig. 4.

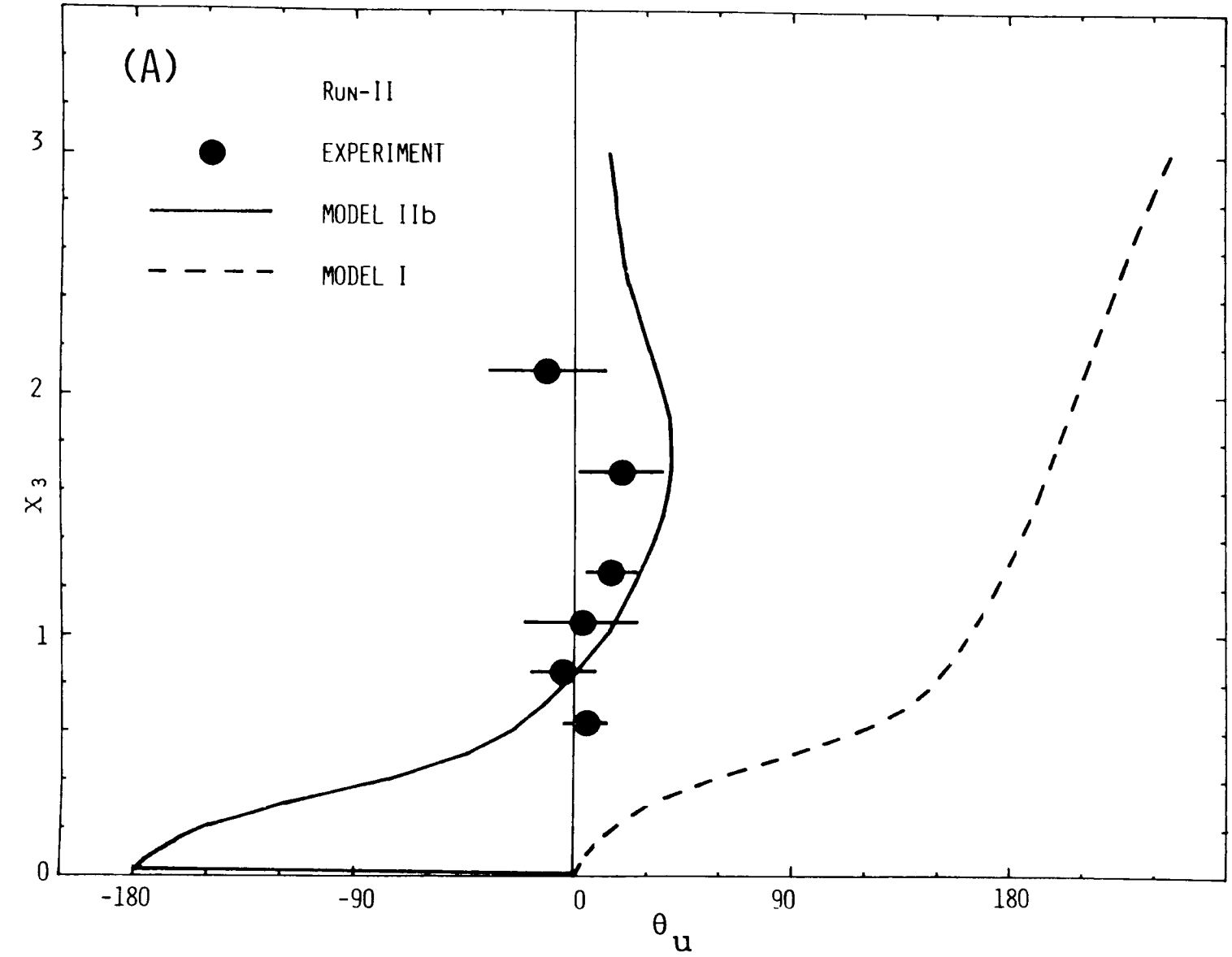
(A)
RUN-II
EXPERIMENT
MODEL IIb
MODEL I
3
2
1
0
x_3
-180
-90
0
90
180
θ_u
7 cm

Fig. 5a.

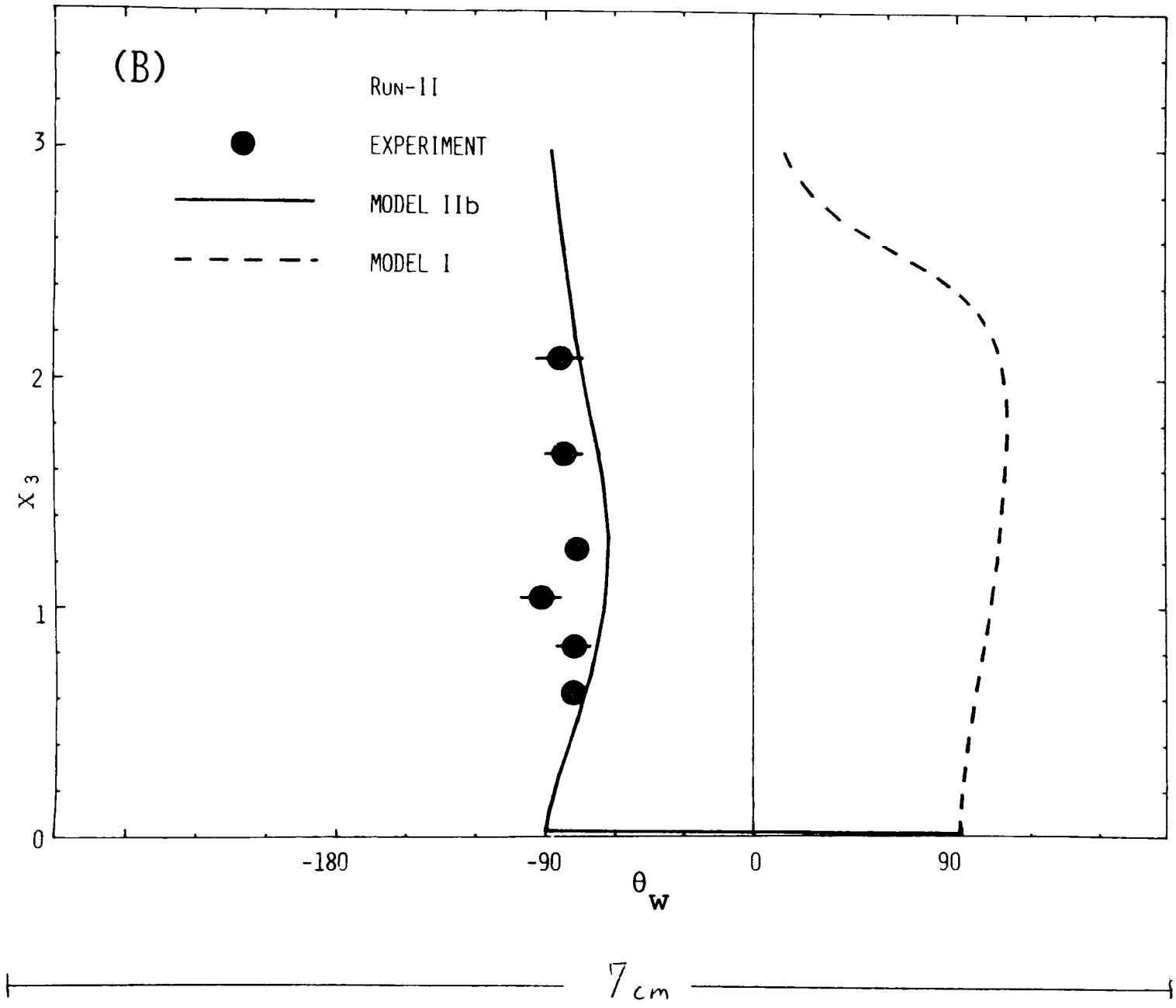
(B)
RUN-II
EXPERIMENT
MODEL IIb
MODEL I
3
2
1
0
X_3
-180
-90
0
90
θ_w
7 cm

Fig 5b.

The Energy Balance in the Wind-wave Spectrum

Hiroshi ICHIKAWA**

Abstract:

The mechanism of the development of wind-wave spectrum is studied with taking into account the energy input from turbulent wind, the energy dissipation due to water turbulence and the energy rearrangement due to nonlinear wave-wave interaction. The energy input from turbulent wind to irrotational wind-waves is estimated in the curvilinear co-ordinates using a turbulent model proposed by ICHIKAWA (1978). The energy dissipation due to water turbulence is assumed to be several times greater than that due to molecular viscosity of water. And then, the nonlinear energy-transfer is estimated from the total energy balance. It is found that the spectral distribution of the nonlinear transfer estimated in this paper is qualitatively equal to that obtained from the nonlinear wave-wave interaction theory. Further more, it is shown that the contribution from nonlinear energy-transfer to the development of wind-waves is large but it becomes small as the amplitude of wind-waves decreases.

The eddy viscosities of air and water are found to change with respect to characteristic height of wind-wave field and friction velocity of air.

** Geophysical Institute, Faculty of Science, Kyoto University, Kitashirakawa Oiwake-cho, Sakyo-ku, Kyoto, 606 Japan

1. Introduction

The growth of wind-waves in ocean is one of the most mysterious problems in Oceanography. Although many theoretical studies have been made, we have not had a good agreement between the theories and the observed results (SNYDER and COX; 1966, BARNETT and WILKERSON; 1967, DOBSON; 1971 and others). Some investigators tried to attribute this discrepancy to the existence of the atmospheric turbulence (YEFIMOV; 1970, DAVIS; 1972, TWONSEND; 1972, FUJINAWA; 1974, GENT and TAYLOR; 1976) and to the nonlinear wave-wave interaction (HASSELMANN et al.; 1973, IMASATO; 1976b and others).

ICHIKAWA (1978) proposed a model on the turbulent wind field over wind-waves, named as Model II in which the turbulent wind field is formulated in the curvilinear co-ordinates. He clearly showed that the wind field over wind-waves calculated numerically from his model has a good agreement with the experimental result of ICHIKAWA and IMASATO (1976) which is different from the wind field predicted by the Miles' (1957) quasi-laminar model. It suggests that the energy input from wind to waves also has to be estimated in the curvilinear co-ordinates with taking into account the atmospheric turbulence. Therefore, in this paper, the energy input from turbulent wind to waves is estimated in the curvilinear co-ordinates using the Model II, but it depends on unknown value of a parameter α representing the rate of increase of the eddy viscosity of air due to underlying wind-waves. We must find a method to determine the most suitable value of α.

On the other hand, IMASATO and ICHIKAWA (1977) measured the velocity fluctuations in water and suggested that the wave energy is dissipated by the water turbulence. Unfortunately, the dissipation of wave energy due to water turbulence has not been clarified yet. Therefore, it is assumed in this paper that the energy dissipation due to water turbulence is β times greater than that due to molecular viscosity of water.

The most suitable values of the parameters α and β can be determined so as to satisfy the condition that the integrations in the frequency domain from zero to infinity of the energy and the momentum transfers due to nonlinear wave-wave interaction must be vanished. After the values of α and β are determined in this way, the spectra of the energy input and the energy dissipation can be obtained, and then, the spectrum of the nonlinear energy transfer can be obtained, using the observed energy flux necessary for the wind-waves to develop.

In this paper, the dependencies of α and β on wind-wave field and friction velocity of air are examined from the evaluation of α and β in the cases of the wind tunnel experiment performed by KUNISHI (1963) and of the JONSWAP-observation. The value of α fixed in this paper is compared with the range of suitable value of α obtained in the previous paper of ICHIKAWA (1978). On the basis of the above results, the spectral energy balance in the wind-wave spectrum in different stage and the contribution from the nonlinear energy-transfer to the development of the wind-wave spectrum are discussed.

2. Momentum and energy inputs from wind to waves

Fig. 1 By the use of the curvilinear orthogonal system of co-ordinates (ξ_1, ξ_2, ξ_3) illustrated in Fig. 1, we consider the momentum and energy inputs from turbulent wind to a component wave which is represented in the Cartesian system of co-ordinates (x_1, x_2, x_3) as follows,

$$x_3 = \zeta = a \cos(k\xi_1) \tag{2.1}$$

which equals $\underline{a} \cos(k(x_1 - Ct))$ to the order of $\underline{ak}$. Here, $\underline{a}$, $\underline{k}$ and $\underline{C}$ are the wave-amplitude, the wave-number and the phase velocity of the component wave, respectively, and $\underline{t}$ the time. The Cartesian system of co-ordinates is also illustrated in Fig. 1. As is described in the previous paper of ICHIKAWA (1978), the wavy boundary surface is expressed in the curvilinear co-ordinates as $\xi_3 = 0$. It is assumed in this paper that the wind field is homogeneous in the ξ_2-direction and $(ak)^2$ is negligibly small.

The total stress S_{nm} denoted in the curvilinear co-ordinates represents the ξ_n-component of total momentum transfer per unit area perpendicular to the ξ_m-axis and is expressed as follows,

$$S_{nm} = -\frac{\langle p \rangle}{\rho_a} \delta_{nm} + r_{nm} + \langle v_{nm} \rangle + w_{nm} \tag{2.2}$$

where p is the static pressure, ρ_a the density of air, δ_{nm} the Kronecker's delta, r_{nm} the turbulent Reynolds stress, v_{nm} the viscous stress and w_{nm} the wave-induced Reynolds stress and the operator $\langle\ \rangle$ represents the phase average denoted by HUSSAIN and REYNOLDS (1970).

It is equal to the time average in the previous paper of ICHIKAWA (1978) at fixed points in a frame of reference travelling with the phase velocity of the component wave. r_{nm} and w_{nm} are denoted as follows,

$$r_{nm} = \langle -u_n' u_m' \rangle \qquad \text{and} \qquad w_{nm} = \langle -\tilde{u}_n \tilde{u}_m \rangle$$

where u_n' and $\tilde{u}_n$ are the turbulent and the wave-induced fluctuations of ξ_n-component of wind velocity, respectively. As the wind field is assumed to be homogeneous in the ξ_2-direction, S_{nm} over wavy boundary is also expressed as follows,

$$S_{nm} = \overline{S}_{nm}(\xi_3) + \tilde{S}_{nm}(\xi_1, \xi_3) \tag{2.3}$$

where $\overline{S}_{nm}$ is the undisturbed part of S_{nm} and $\tilde{S}_{nm}$ the wave-induced periodic part, respectively. $\tilde{S}_{nm}$ is expressed as follows,

$$\tilde{S}_{nm}(\xi_1, \xi_3) = \mathcal{R}_e \{ \hat{S}_{nm}(\xi_3) \exp(jk\xi_1) \} \tag{2.4}$$

taking the first term of the Fourier series expansion of $\tilde{S}_{nm}$. Here, $\mathcal{R}_e$ denotes the real part of a complex variable, $\hat{S}_{nm}$ is the complex amplitude of $\tilde{S}_{nm}$ and $j = \sqrt{-1}$.

The mean stress $[\overline{S}_{n3}]_\zeta$ right at the wavy surface represents the transfer of the ξ_n-component of momentum from wind to mean motion in water and only the wave-induced periodic part $[\tilde{S}_{n3}]_\zeta$ represents that from wind to waves per unit area at the wavy surface perpendicular to ξ_3-axis. Therefore, the x_1-component of momentum input F^M_{inp} and the energy input F^E_{inp} from turbulent wind to waves per unit

horizontal area can be represented as follows, respectively,

$$F^{M}_{inp} = \rho_a \overline{[M_{1m}\tilde{S}_{m3}]_\zeta A} \tag{2.5}$$

$$F^{E}_{inp} = \rho_a \overline{[\langle v_n \rangle M_{nm}\tilde{S}_{m3}]_\zeta A} \tag{2.6}$$

where the overbar denotes the average over several waves along the wavy surface and A is the projected area on the x_1x_2-plane of the unit area at the wavy surface perpendicular to ξ_3-axis. M_{nm} is the matrix by which the unit vectors of ξ_1, ξ_2 and ξ_3-axes are transformed into the unit vector of x_n-axis and $\langle v_n \rangle$ is the phase average of x_n-component of wind velocity. $[M_{nm}]_\zeta$ and A, which are correct to the order of $(ak)^2$, are represented as follows,

$$[M_{nm}]_\zeta = \begin{pmatrix} 1 - \frac{1}{2}(\frac{\partial}{\partial x_1}\zeta)^2, & 0, & -\frac{\partial}{\partial x_1}\zeta \\ 0, & 1, & 0 \\ \frac{\partial}{\partial x_1}\zeta, & 0, & 1 - \frac{1}{2}(\frac{\partial}{\partial x_1}\zeta)^2 \end{pmatrix}$$

$$A = 1 - \frac{1}{2}(\frac{\partial}{\partial x_1}\zeta)^2$$

From the boundary conditions that the mass flux through the water surface must be vanished and that the air particle does not slip relatively to the water particle at the water surface, it is derived as follows,

$$[\langle v_3 \rangle]_\zeta = \{[\bar{v}_c]_\zeta - c\} \frac{\partial}{\partial x_1}\zeta$$

$$[\langle v_1 \rangle]_\zeta = [\bar{v}_c]_\zeta + kc\zeta + [\tilde{v}_c]_\zeta$$

where $[\bar{v}_c]_\zeta$ is the mean horizontal velocity of water along the wavy water surface, $kC\zeta$ the orbital velocity of wave at the water surface and $[\tilde{v}_c]_\zeta$ the additional periodic fluctuation of horizontal velocity of water produced at the wavy surface by $[\tilde{S}_{13}]_\zeta$. Therefore, the x_1-component of momentum input F^M_{inp} and the energy input F^E_{inp} from turbulent wind to waves which are correct to the order of $(ak)^2$, can be represented as follows,

$$F^M_{inp} = -\rho_a \overline{[\tilde{S}_{33}]_\zeta \frac{\partial}{\partial x_1}\zeta} \tag{2.7}$$

$$F^E_{inp} = -\rho_a C\overline{[\tilde{S}_{33}]_\zeta \frac{\partial}{\partial x_1}\zeta} + \rho_a kC\overline{[\tilde{S}_{13}]_\zeta \zeta} + \rho_a\overline{[\tilde{v}_c \tilde{S}_{13}]_\zeta} \tag{2.8}$$

It is apparent that $[\tilde{S}_{13}]_\zeta$ does not transfer directly the momentum from wind to waves as shown by Eq.(2.7). On the other hand, LONGUET-HIGGINS (1969) showed that the momentum is indirectly transfered from wind to waves by $[\tilde{S}_{13}]_\zeta$ through the additional pressure fluctuation δp which is associated with the variation of the thickness of the boundary layer produced in water by $[S_{13}]_\zeta$. According to him, δp is represented as follows,

$$\delta p = \mathcal{R}_e\{ j \hat{S}_{13}(0) \exp(jk\xi_1)\}$$

Therefore, F^M_{inp} in Eq.(2.7) is rewriten as follows,

$$\begin{aligned} F^M_{inp} &= -\rho_a \overline{[\tilde{S}_{33}]_\zeta \frac{\partial}{\partial x_1}\zeta} + \rho_a \overline{\delta p \frac{\partial}{\partial x_1}\zeta} \\ &= -\rho_a \overline{[\tilde{S}_{33}]_\zeta \frac{\partial}{\partial x_1}\zeta} + \rho_a k \overline{[\tilde{S}_{13}]_\zeta \zeta} \end{aligned} \tag{2.9}$$

In this paper, it is assumed that $[\tilde{v}_c]_\zeta$ is negligibly small

compared with $kC\zeta$ as assumed in the Model II proposed by ICHIKAWA (1978). Therefore, the following relation is derived from Eqs.(2.8) and (2.9),

$$F^{E}_{inp} = C\, F^{M}_{inp} \tag{2.10}$$

Since the energy density E of irrotational wave equals CM (M ; the momentum density of irrotational wave), F^{E}_{inp} and F^{M}_{inp} can be represented as follows, respectively,

$$F^{E}_{inp} = \frac{\rho_a}{\rho_w}\, k\, C\, \hat{F}_{inp}\, E \tag{2.11}$$

$$F^{M}_{inp} = \frac{\rho_a}{\rho_w}\, k\, C\, \hat{F}_{inp}\, M \tag{2.12}$$

where ρ_w is the density of water and $\hat{F}_{inp}$ is the non-dimensional input denoted as follows,

$$\hat{F}_{inp} = \frac{2}{k^2 a^2 C^2} \left\{ - \overline{[\tilde{S}_{33}]_\zeta \frac{\partial}{\partial x_1}\zeta} + k\, \overline{[\tilde{S}_{13}]_\zeta \zeta} \right\} \tag{2.13}$$

In this paper, the value of $\hat{F}_{inp}$ is numerically calculated from the Model II. The assumptions adopted in this model are briefly described in Apendix. It must be emphasized that $\hat{F}_{inp}$ calculated from the model II depends on the value of α representing the rate of increase of the eddy viscosity of air due to underlying wind-waves because the wind field calculated from the Model II depends on the value of α as shown in the previous paper of ICHIKAWA (1978).

3. Momentum and energy balances

At each frequency of the wave spectrum, the net energy source

function F^E_{net} can be evaluated from the observation of the development of wind-wave spectrum as follows,

$$F^E_{net}(f) = \frac{\partial}{\partial t} E(f) + C_g(f) \frac{\partial}{\partial x_1} E(f) \qquad (3.1)$$

where C_g is the group velocity of the component wave and E the spectral density of wave energy.

F^E_{net} is considered to be decomposed into the energy input F^E_{inp} from wind to waves, the energy transfer F^E_{nol} due to nonlinear wave-wave interaction and the energy dissipation F^E_{dis} due to water turbulence; i.e.,

$$F^E_{net}(f) = F^E_{inp}(f) + F^E_{nol}(f) + F^E_{dis}(f) \qquad (3.2)$$

The purpose of this paper is to examine the contribution from each source functions in the right-hand side of Eq.(3.2) to the net source function F^E_{net} obtained from the observation.

$F^E_{inp}(f)$ can be estimated from Eq.(2.11) by the use of the Model II. However, in the estimation of the spectral distribution of $F^E_{inp}(f)$, it must be taken into account that the wave-induced fluctuations of wind velocities in the frequecy region except near the frequency f_p of the wave spectral peak are fairly small compared with the background atmospheric turbulence (see Fig. 3 in ICHIKAWA and IMASATO (1976)). IMASATO (1976b) suggested that the influence of the corrugation of wavy surface to the wind field over wind-waves will be dominant only in the frequency region near the peak frequency and that the energy is transfered from wind only to the steepest component waves near

the peak frequency, i.e., the wind-wave field receives the energy from wind through a kind of filter associated with the wave steepness. However, the functional form of the filter has not been clarified yet. Therefore, it is assumed in this paper that the filtering function $\phi(f/f_p)$ is represented by Eq.(3.3) and that $F^E_{inp}(f)$ in Eq.(2.11) is rewriten by Eq.(3.4).

$$\phi(f/f_p) = \begin{cases} \cos^2\left(\frac{\pi}{3}(f/f_p - 1)\right), & f \leqq 2.5\ f_p \\ 0, & f > 2.5\ f_p \end{cases} \tag{3.3}$$

$$F^E_{inp}(f) = \frac{\rho_a}{\rho_w} k(f)\ C(f)\ \phi(f/f_p)\ \hat{F}_{inp}(\alpha, f)\ E(f) \tag{3.4}$$

In Eq.(3.4), the parameter α on which $\hat{F}_{inp}$ depends is assumed to be constant with respect to the frequency f of the component wave. The form of $\phi(f/f_p)$ is introduced so as that $\phi(f/f_p)$ equals unity at $f = f_p$ and it gradualy changes to zero at $f = 2.5\ f_p$ where the power spectral density of wind-waves is negligibly small compared with that at $f = f_p$.

The dissipation of wave energy due to water turbulence has not been clarified yet. Therefore, it is assumed that waves dissipate their energy due to the eddy viscosity of water and the eddy viscosity is β times greater than the molecular viscosity ν_w of water. Therefore, $F^E_{dis}(f)$ is represented as follows,

$$F^E_{dis}(f) = -4\beta\ \nu_w\ k^2(f)\ E(f) \tag{3.5}$$

where the parameter β is assumed to be constant with respect to

the frequency of the component wave. As the relation $E(f) = C(f)\, M(f)$ is satisfied for the irrotational wave as described in the section 2, the following relations can be derived,

$$F^M_{net}(f) = F^E_{net}(f) \,/\, C(f) \tag{3.6}$$

$$F^M_{dis}(f) = F^E_{dis}(f) \,/\, C(f) \tag{3.7}$$

where F^M_{net} is the net source function of x_1-component of momentum and F^M_{dis} the momentum dissipation due to water turbulence. As same as F^E_{net} in Eq.(3.2), F^M_{net} is represented as follows,

$$F^M_{net}(f) = F^M_{inp}(f) + F^M_{nol}(f) + F^M_{dis}(f) \tag{3.8}$$

where F^M_{nol} is the x_1-component of momentum transfered nonlinearly from other spectral components to the component wave of frequency f.

As the integrations of F^M_{nol} and F^E_{nol} in the frequency domain from f = 0 to infinity must be vanished, it is derived from Eqs.(3.2) and (3.8) as follows,

$$\int_0^\infty F^M_{net}(f)\, df = \int_0^\infty F^M_{inp}(f)\, df + \int_0^\infty F^M_{dis}(f)\, df \tag{3.9}$$

$$\int_0^\infty F^E_{net}(f)\, df = \int_0^\infty F^E_{inp}(f)\, df + \int_0^\infty F^E_{dis}(f)\, df \tag{3.10}$$

Using Eqs.(3.1), (3.4) and (3.5), the parameter α can be fixed together with the parameter β so as to satisfy Eqs.(3.9) and (3.10). Therefore, $F^E_{inp}(f)$, $F^E_{dis}(f)$ and $F^E_{nol}(f)$ can be evaluated at each frequency from Eqs.(3.4), (3.5) and (3.2), respectively. The upper limit of the integrations in Eqs.(3.9) and (3.10) is taken to

be as five times greater than the frequency f_p of the wave spectral peak because the contribution from the source functions in the frequency region higher than $5f_p$ to the integrations are vanished or very small.

4. Wave data

In this paper, the wave data of the wind tunnel experiment performed by KUNISHI (1963) and of the JONSWAP-observation are used in the estimation of α and β. In the case of wind tunnel experiment, the estimation is performed at the middle point of the two observation points. In order to obtain the wave spectrum at the middle point, which is necessary to estimate the energy and momentum balances, the following procedure is adopted. The power spectra P(f) of wind-waves at the two observation points are expressed by the least-square fitted analytic function proposed by HASSELMANN et al. (1973) as follows,

$$P(f) = \alpha_H g^2 (2\pi)^{-4} f^{-5} \exp\left(-\frac{5}{4}\left(\frac{f}{f_p}\right)^{-4}\right) \gamma^{\exp\left(-\frac{(f-f_p)^2}{2\sigma^2 f_p^2}\right)}, \tag{4.1}$$

where

$$\sigma = \begin{cases} \sigma_a, & \text{for} \quad f \leqq f_p, \\ \sigma_b, & \text{for} \quad f > f_p. \end{cases}$$

Here, g is the acceleration of gravity and f_p, α_H, γ, σ_a and σ_b are the shape parameters determined from the experimental data. Then, the wave spectrum at the middle point is estimated by Eq.(4.1) with the shape parameters which are determined by interpolation using the shape parameters at the two observation points.

In the case of the JONSWAP-observation, the similarity law on the shape of the wave spectrum proposed by HASSELMANN et al. (1973) is adopted, i.e., the power spectrum of wind-waves is represented by Eq.(4.1) with constant values of $\gamma = 3.3$, $\sigma_a = 0.07$ and $\sigma_b = 0.09$ and the parameters f_p and α_H changing with respect to fetch X as follows,

$$f_p = 3.5 \frac{g}{U_{10}} (Xg / U_{10}^2)^{-0.33} \tag{4.2}$$

$$\alpha_H = 0.076 (Xg / U_{10}^2)^{-0.22} \tag{4.3}$$

where U_{10} is the mean wind velocity at the height of 10 m.

The net energy source function $F^E_{net}(f)$ denoted by Eq.(3.1) is evaluated according to HASSELMANN et al. (1973) as follows,

$$F^E_{net}(f) = \rho_w C_g(f) k(f) C^2(f) \sum_{n=1}^{5} \frac{\partial}{\partial x_1} a_n \frac{\partial}{\partial a_n} P(f) \tag{4.4}$$

where $a_1, a_2, \ldots a_5$ are the shape parameters f_p, α_H, γ, σ_a and σ_b, respectively. It must be noticed that the term of local time change in Eq.(3.1) is vanished because the wave spectrum is stationary in the wind tunnel experiment and the wave spectrum in the case of JONSWAP-observation changes only with respect to fetch as shown by Eqs.(4.2) and (4.3).

5. Results and discussion

The parameter α represents the rate of increase of the atmospheric eddy viscosity due to underlying wind-wave field and the parameter β represents the rate of increase of the dissipation due

to water turbulence which is produced by the wave motion and the shear flow in water. Therefore, the parameters α and β are conjectured to change with respect to conditions of wind-wave field and background turbulences in air and water. Since the power spectrum P(f) of wind-waves expressed by Eq.(4.1) is rewriten as follows,

$$P(f) = \psi (f/f_p)\ P(f_p)$$

where $\psi(f/f_p)$ is a non-dimensional function, the integration of P(f) is represented as follows,

$$\int_0^\infty P(f)\ df = I\ f_p\ P(f_p)$$

where

$$I = \int_0^\infty \psi(f/f_p)\ d(f/f_p)$$

which is insensible to the shape parameters denoted in Eq.(4.1). As the value of $\underline{I}$ is nearly constant, the wind field can be characterized by the height H_s which is denoted by $H_s = \sqrt{f_p\ P(f_p)}$. The atmospheric background turbulence is characterized by the friction velocity u_* of air. The water turbulence produced by shear flow in water is characterized by the friction velocity of water which equals $0.03\ u_*$. Therefore, it can be conjectured that both of the parameters α and β depend on the non-dimensional wave-height H* and the non-dimensional friction velocity u_** of air which are denoted as follows, respectively,

$$H^* = \frac{H_s u_*}{\nu_a} \qquad \text{and} \qquad u_*^* = \left(\frac{u_*^3}{\nu_a g} \right)^{1/3}$$

where ν_a is the kinematic molecular viscosity of air.

In this paper, the parameters α and β are evaluated in the case of wind tunnel experiment performed by KUNISHI (1963) and the case of JONSWAP-observation in order to examine the dependencies of α and β on H^* and u_*^*. The results of the evaluation are tabulated in Table 1 together with the conditions of mean wind velocity profile and the shape parameters of wind-wave spectrum. The values of $u_*^{*2}\alpha$ and $u_*^*(\beta - 1)$ are plotted against H^* in Figs. 2 and 3, respectively. From these figures, it can be recognized that the parameters α and β are well expressed by Eqs.(5.1) and (5.2), respectively.

$$\alpha = A_\alpha H^{*p_\alpha} u_*^{*-2} \tag{5.1}$$

$$\beta = 1 + A_\beta H^{*p_\beta} u_*^{*-1} \tag{5.2}$$

The values of the coefficients A_α, A_β, p_α and p_β are tabulated in Table 2. It must be mentioned here that the values of α and β plotted in the figures are only for the wave spectra in the "stage of sea-waves" and those in the "transition stage" defined by IMASATO (1976a) because it is found that the Model II can not explain the measured wind field over wind-waves in the "stage of initial-wavelets". The reason seems that the steepness of initial-wavelets is very small and the wind speed over them is very weak, and another mechanism must be introduced as suggested by IMASATO (1976b).

In Fig. 2 are also shown the ranges of the suitable value of α obtained in the previous paper of ICHIKAWA (1978) for the experimental

cases of Run-I, II and III, respectively. These ranges were determined so as that the Model II could explain well the measured wind field over wind-waves. It is apparent that the value of α evaluated from the present method agrees with that obtained in the previous paper (ICHIKAWA, 1978) for the same value of H*. It indicates that the Model II predict well not only the turbulent wind field over wind-waves but also the energy input necessary for the underlying wind-waves to develop.

It is seen in Fig. 2 that the values of p_α in the "stage of sea-waves" and the "transition stage" are different from each other. This result suggests that the value of p_α is associated with the wave-steepness because the wave-steepness changes with respect to H* in the "transition stage" and it has a fairly constant value in the "stage of sea-waves" as shown by KUNISHI (1963).

On the other hand, p_β may not be associated with the wave-steepness because the values of p_β in the "stage of sea-waves" and in the "transition stage" are equal to each other. As p_β has a constant value of unity in the case of wind tunnel experiment, the parameter β in this case can be represented only by the characteristic height H_s of wind-wave field as follows,

$$\beta = 1 + 0.213 \left(\frac{g}{\nu_a^2}\right)^{1/3} H_s$$

Therefore, the water turbulence in the wind tunnel can be largely attributed to the wave motion in water. On the other hand, the value of p_β in the case of the JONSWAP-observation is greater than

unity. This suggests that the parameter β in this case becomes large not only as H_s but also as u_* becomes large. Therefore, it seems likely that the water turbulence produced by shear flow in water in the case of the JONSWAP-observation is too intense to be neglected comparing with the water turbulence produced by wave motion. It must be noticed in Table 1 that the large wind-waves have a large value of β to reach to fourty, i.e., they dissipate far larger energy due to the water turbulence than due to the molecular viscosity. This result may offer a suggestion to the problem of the rapid decay of wind-waves in the region out of the storm area.

It is concluded that the representations of the eddy viscosities of air and water using the parameters α amd β are useful to parametarize the influence of wave motion to turbulence in air and water because α and β can be determined by H* and u_**. It must be mentioned here that the discrepancies between the values of α and β in the wind tunnel experiment and those in the JONSWAP-observation remain to be explained.

Now, we proceed to discuss the spectral energy balance in a wind-wave spectrum obtained from the method described in the section 3. Figs. 4, 5 and 6 show the spectral distributions of F^E_{net}, F^E_{inp}, F^E_{nol} and F^E_{dis} in the cases of JRUN-1e, KRUN-19b and KRUN-13b, respectively. The wave spectra of JRUN-1e and KRUN-19b belong to the "stage of sea-waves" and the wave spectrum of KRUN-13b belongs to the "transition stage".

It must be emphasized that the spectral distribution of $F^E_{nol}(f)$

shown in these figures are similar to that calculated theoretically by HASSELMANN et al. (1973), i.e., they have a negative lobe in the frequency region higher than the frequency f_p of the wave spectral peak and two positive lobes in the frequency regions lower than f_p and much higher than f_p, respectively. According to HASSELMANN et al. (1973), the non-dimensional function $\hat{F}_{nol}(f/f_p)$ denoted by Eq.(5.3) has a unique spectral distribution for a family of wave spectra which are self-similar in shape,

$$\hat{F}_{nol}(f/f_p) = \rho_w^{-1} \alpha_H^{-3} g^{-3} f_p^4 F^E_{nol}(f) \qquad (5.3)$$

Since the wave spectra adopted in this paper for the case of JONSWAP-observation are self-similar in shape as suggested by HASSELMANN et al. (1973), $\hat{F}_{nol}$ in this case must be independent of the parameters α and β.

Fig. 7 shows the function $\hat{F}_{nol}$ estimated from the present method for the family of the JONSWAP-spectra used in this paper. It is apparent that the spectral distributions of $\hat{F}_{nol}$ calculated from the present method for the JONSWAP-spectra in different conditions of mean wind velocity and fetch are nearly equal to each other. In Fig. 7 is also shown the theoretical $\hat{F}_{nol}$ which is obtained from the theoretical $F^E_{nol}(f)$ in Fig. 2.12 in HASSELMANN et al. (1973). It is found that $\hat{F}_{nol}$ estimated from the present method qualitatively agrees well with the theoretical $\hat{F}_{nol}$ corresponding to theoretical $F^E_{nol}(f)$ calculated by HASSELMANN et al. (1973). From these results, it could be concluded that the nonlinear transfer of wave energy

estimated from the present method concerning with the turbulence in air and water can be largely attributed to the nonlinear energy transfer predicted by the Hasselmann's (1962) nonlinear wave-wave interaction theory.

On the other hand, in the case of wind tunnel experiment, the theoretical calculation of F^E_{nol} using the nonlinear wave-wave interaction theory has a rather difficult problem, i.e., the influence of the surface tension to the dispersion relation of water waves in the wind tunnel is too large to be neglected and the calculation method proposed by HASSELMANN (1963) can not be used. Therefore, we can not compare the calculated F^E_{nol} in this paper with the theoretical F^E_{nol}. However, the spectral distribution of F^E_{nol} shown in Fig. 6 is similar to that shown in Fig. 2.21(d) of HASSELMANN et al. (1973) which is calculated theoretically for the wave spectrum of which peak is much narrower than that of the mean JONSWAP-spectrum. This result suggests that F^E_{nol} estimated in this paper must agree with the theoretical F^E_{nol} also in the case of wind tunnel experiment because the peak of the wave spectrum in this case is much narrower than that of the mean JONSWAP-spectrum. It is concluded that the present method is appropriate to estimate the spectral distribution of F^E_{nol}.

It is apparent in Figs. 4, 5 and 6 that F^E_{inp} estimated in this paper is dominant arround the frequency f_p of the wave spectral peak. This result agrees with the Imasato's (1976b) model in which the dominant and steepest component waves are assumed to receive the almost whole amount of momentum necessary for wind-waves to develop.

It must be noticed in Fig. 4 that F^E_{dis} in the case of JRUN-1e is negligibly small compared with other source functions and that F^E_{net} in this case can be largely attributed to F^E_{nol} which agrees with the conclusion of HASSELMANN et al. (1973). On the other hand, F^E_{dis} in the case of KRUN-13b can not be neglected compared with other source functions and F^E_{net} in this case can be attributed not only to F^E_{nol} but also to F^E_{inp}. It can be concluded that the contribution from F^E_{nol} to F^E_{net} becomes small as the amplitude of wind-waves becomes small although F^E_{nol} can not be neglected in any case.

It must be mentioned at last that it is the total stress which transfers the momentum from wind to waves although it has been thought since MILES (1957) that only the pressure fluctuation at the wave surface transfers it from wind to waves. DAVIS (1972) also estimated the momentum input by total stress and showed that the total stress could not increase the momentum of a purely irrotational wave. On the other hand, it is found in this paper that the total stress can increase the wave momentum because F^M_{inp} calculated from Eq.(2.12) has a positive value. This discrepancy can be attributed to the adopted co-ordinates systems. In the Cartesian co-ordinates adopted by DAVIS (1972), the total stress can not be estimated right at the wavy surface and it is determined only at the mean water surface level by the Taylor series expansion. On the other hand, since the total stress can be precisely estimated right at the wave surface in the curvilinear co-ordinates, F^M_{inp} can be precisely estimated from Eq.(2.9) in this system of co-ordinates. It must be emphasized that

the momentum input from turbulent wind to waves must be estimated in the curvilinear co-ordinates.

Acknowlegements

The author wishes to express his thanks to Prof. H. KUNISHI of Kyoto University for his discussion and encouragement. He also expresses his gratitude to Dr. N. IMASATO of Kyoto University for his critical discussion throughout this study. The numerical calculations in this article were carried out on a FACOM M-190 in the Data Processing Center of Kyoto University.

References

BARNETT, T.P. and J.C. WILKERSON (1967): On the generation of ocean wind waves as inferred from airborn radar measurements of fetch-limited spectra. J. Mar. Res., 25, 292-328.

DAVIS, R.E. (1972): On the prediction of the turbulent flow over a wavy boundary. J. Fluid Mech., 52, 287-306.

DOBSON, F.W. (1971): Measurements of atmospheric pressures on wind-genarated sea waves. J. Fluid Mech., 48, 225-274.

FUJINAWA, Y. (1974): A model on the mechanism of momentum transfer from turbulent atmospher to water waves. J. Oceanogr. Soc. Japan, 30, 97-107.

GENT, P.R. and P.A. TAYLOR (1976): A numerical model of the air flow above water waves. J. Fluid Mech., 77, 105-128.

HASSELMANN, K. (1962): On the non-linear energy transfer in a gravity-wave spectrum, Part 1. General theory. J. Fluid Mech., 12, 481-500.

HASSELMANN, K. (1963): On the non-linear energy transfer in a gravity-wave spectrum, Part 3. Evaluation of the energy flux and swell-sea interaction for a Neumann spectrum. J. Fluid Mech., 15, 385-398.

HASSELMANN, K., T.P. BARNETT, E. BOUWS, H. CARLSON, D.E. CARTWRIGHT, K. ENKE, J.A. EWING, H. GIENAPP, D.E. HASSELMANN, P. KRUSEMAN, A. MEERBURG, P. MÜLLER, D.J. OLBERS, K. RICHTER, W. SELL and H. WALDEN (1973): Measurements of wind-wave growth and swell decay during the Joint North Sea Wave Project (JONSWAP).

Ergänzungscheft zur Deutschen Hydrographischen Zeitschrift, Reihe A (8°), 12, 1-95.

HUSSAIN, A.K.M.F. and W.C. REYNOLDS (1970): The mechanics of an organized wave in turbulent shear flow. J. Fluid Mech., 41, 241-258.

ICHIKAWA, H. and N. IMASATO (1976): The wind field over wind-waves. J. Oceanogr. Soc. Japan, 32, 271-283.

ICHIKAWA, H. (1978): A model on the turbulent wind field over wind-waves in curvilinear co-ordinates. J. Oceanogr. Soc. Japan, 34, (in press).

IMASATO, N. (1976a): Some characteristics of the development process of the wind-wave spectrum. J. Oceanogr. Soc. Japan, 32, 21-32.

IMASATO, N. (1976b): The mechanism of the development of wind-wave spectra. J. Oceanogr. Soc. Japan, 32, 253-266.

IMASATO, N. and H. ICHIKAWA (1977): Nonlinearity of the horizontal velocity field under wind-waves. J. Oceanogr. Soc. Japan, 33, 61-66.

KUNISHI, H. (1963): An experimental study on the generation and growth of wind waves. Bull. Disast. Prev. Res. Inst., Kyoto Univ., 61, 1-41.

LONGUET-HIGGINS, M.S. (1969): Action of a variable stress at the surface of water waves. The Physics of Fluid, 12, 737-740.

MILES, J.W. (1957): On the generation of surface waves by shear flows. J. Fluid Mech., 3, 185-204.

SNYDER, R.L. and C.S. COX (1966): A field study of the wind generation of ocean waves. J. Mar. Res., 24, 141-178.

TOWNSEND, A.A. (1972): Flow in a deep turbulent boundary layer over a surface distorted by water waves. J. Fluid Mech., 55, 719-735.

YEFIMOV, V.V. (1970): On the structure of the wind velocity field in the atmospheric near-water layer and the transfer of wind energy to sea waves. Izv. Atmos. Oceanic Physics, 6, 1043-1058.

Apendix

The assumptions adopted in the Model II are as briefly described bellow although they are described in the previous paper of ICHIKAWA (1978).

1) The wind field is homogeneous in the ξ_2-direction and the mean wind velocity has only the ξ_1-component $\bar{u}_1$, i.e.,

$$\bar{u}_1(\xi_3) = \begin{cases} \frac{u_*}{\kappa} \ln(\xi_3 / z_0) - C, & \xi_3 \geqq z_1 \\ \frac{u_*}{\kappa} \frac{\Delta U}{z_1} \xi_3 - C, & \xi_3 < z_1 \end{cases}$$

where κ is the Kármán constant, u_* the friction velocity of air, z_0 the roughness height, ΔU the thickness parameter of "linear sublayer" and z_1 equals $z_0 \exp(\Delta U)$.

2) The slope of the underlying component wave is so small as the wave-induced Reynolds stress w_{nm} is negligibly small compared with the turbulent Reynolds stress r_{nm}.

3) The wave-induced variations of turbulent Reynolds stresses are expressed as follows,

$$\tilde{r}_{11} = \tilde{r}_{33} \qquad \text{and} \qquad \tilde{r}_{13} = \alpha \nu_s \tilde{e}_{13}$$

where α is a non-dimensional parameter with a positive constant value, $\tilde{e}_{13}$ the wave-induced variation of tangential rate-of-strain and ν_s the eddy viscosity associated with the vertical shear of mean wind velocity.

4) The boundary conditions for the wave-induced fluctuations of ξ_n-component of wind velocity in a frame of reference travelling

with the phase velocity of the component wave are represented as follows,

$$[\tilde{u}_1]_\zeta = k\,C\,\zeta\,, \qquad [\tilde{u}_3]_\zeta = 0,$$

$$[\tilde{u}_1]_H = 0 \qquad \text{and} \qquad [\tilde{u}_3]_H = 0$$

where subscripts ζ and H denote the values at the wavy boundary surface and at the height sufficiently far from the wave surface, respectively.

In this paper, the value of ΔU is chosen so as that the "linear sublayer" is coincident with the viscous sublayer when the parameter $D = \kappa u_* z_0 / \nu_a$ is smaller than exp(-1) and is chosen to be unity when the parameter D is greater than exp(-1).

風波のスペクトルにおける
エネルギーバランス

市川　洋**

要旨：乱れた風から風波へのエネルギー流入，成分波間の非線形相互作用によるエネルギーの再分配，水中の乱れによるエネルギー逸散を考慮に入れて風波のスペクトルの発達機構を調べた。乱れた風から風波（渦なし）へのエネルギー流入はICHIKAWA(1978)が提案した乱流モデルを用いて曲線座標系で求めた。水中の乱れによるエネルギー逸散は分子粘性による逸散の定数倍と仮定して求めた。その後で非線形相互作用によるエネルギー輸送量を全エネルギーの釣合いから求めた。このようにして得られたエネルギーの非線形輸送量の周波数分布は成分波間の非線形相互作用の理論から得られるものと定性的に一致することが見出された。更に風波のスペクトルの発達へのエネルギー非線形輸送の寄与は大きいが，それは風波の振巾の減少とともに小さくなるこ

とが示される。

空気と水の渦粘性係数は風波の場の特性高さと空気の摩擦速度とともに変化することが見出された。

** 京都大学理学部地球物理学教室，〒606
京都市左京区北白川追分町.

Table 1. Values of α and β and the conditions of the vertical profile of mean wind velocity, the fetch and the wind-wave spectrum.

Table 2. Coefficients A_α, p_α, A_β and p_β in Eqs.(5.1) and (5.2).

Fig. 1. Curvilinear orthogonal system of co-ordinates (ξ_1, ξ_2, ξ_3) and Cartesian system of co-ordinates (x_1, x_2, x_3).

Fig. 2. αu_*^{*2} versus H*. The relation of Eq.(5.1) is shown by solid lines.

Fig. 3. $(\beta - 1)u_*^*$ versus H*. The relation of Eq.(5.2) is shown by solid lines.

Fig. 4. Spectral energy balance in the case of JRUN-1e. The thin solid line shows the power spectrum of wind-waves and the thick solid line shows the net energy source function obtained from the observation using Eq.(4.4).

Fig. 5. Spectral energy balance in the case of KRUN-19b.

Fig. 6. Spectral energy balance in the case of KRUN-13b.

Fig. 7. Non-dimensional function $\hat{F}_{nol}(f/f_p)$ calculated for the all wind-wave spectra of JONSWAP-observation used in this paper. The thick solid line shows the theoretical $\hat{F}_{nol}(f/f_p)$ obtained by HASSELMANN et al. (1973).

RUN No.	Fetch (m)	U_{10} (m s^{-1})	u_* (cm s^{-1})	f_p (Hz)	α_H x10^3	γ	H*	α	β	Mark in Figs. 2 and 3
KRUN-14a	7.0	5.99	22.3	7.33	3.07	9.87	6.36	2.06	1.42	
KRUN-15a	7.0	7.02	26.9	6.50	5.33	11.8	1.41×10^1	1.55	1.81	
KRUN-16a	7.0	9.42	38.0	5.30	8.55	8.48	3.21×10^1	0.89	2.23	
KRUN-17a	7.0	10.9	44.9	4.25	8.34	8.27	5.78×10^1	0.83	2.70	▲
KRUN-18a	7.0	12.5	50.2	3.42	11.9	7.04	1.10×10^2	0.94	2.78	
KRUN-19a	7.0	15.2	65.7	3.08	13.2	6.13	1.74×10^2	0.75	5.01	
KRUN-20a	7.0	21.3	99.1	2.80	33.5	5.41	4.77×10^2	0.34	6.00	
KRUN-13b	1.24×10^1	3.85	13.6	6.17	1.13	22.5	5.05	3.04	1.20	
KRUN-14b	1.24×10^1	5.19	19.3	4.67	3.54	15.6	1.84×10^1	3.00	2.06	
KRUN-15b	1.24×10^1	6.49	24.9	4.00	4.30	19.9	4.03×10^1	2.70	3.65	
KRUN-16b	1.24×10^1	8.61	34.7	3.17	6.54	9.40	7.61×10^1	1.49	4.11	
KRUN-17b	1.24×10^1	10.2	41.9	3.00	8.78	11.3	1.30×10^2	1.48	4.54	△
KRUN-18b	1.24×10^1	12.0	46.8	2.58	11.1	7.63	1.81×10^2	1.49	5.01	
KRUN-19b	1.24×10^1	14.3	58.8	2.25	11.2	7.22	2.29×10^2	1.33	7.17	
KRUN-20b	1.24×10^1	21.3	99.2	2.10	33.0	4.99	8.09×10^2	0.91	11.7	
JRUN-1a	1.69×10^2	9.0	40.3	1.41	39.1	3.30	6.45×10^2	1.06	1.43	
JRUN-1b	8.00×10^2	9.0	40.3	0.84	27.8	3.30	1.52×10^3	1.65	3.40	
JRUN-1c	1.69×10^3	9.0	40.3	0.66	23.6	3.30	2.30×10^3	2.00	5.67	●
JRUN-1d	8.00×10^3	9.0	40.3	0.39	16.7	3.30	5.39×10^3	4.00	16.5	
JRUN-1e	1.83×10^4	9.0	40.3	0.30	14.0	3.30	8.51×10^3	6.09	30.3	
JRUN-2a	1.69×10^2	12.0	53.7	1.28	44.4	3.30	1.12×10^3	0.87	2.32	
JRUN-2b	8.00×10^2	12.0	53.7	0.76	31.5	3.30	2.61×10^3	1.23	5.19	
JRUN-2c	1.69×10^3	12.0	53.7	0.60	26.7	3.30	3.98×10^3	1.50	8.71	○
JRUN-2d	8.00×10^3	12.0	53.7	0.36	19.0	3.30	9.33×10^3	2.55	25.6	
JRUN-2e	1.69×10^4	12.0	53.7	0.28	16.1	3.30	1.41×10^4	3.50	42.2	
Run-I	1.90×10^1	3.66	9.39	3.60	—	—	1.32×10^1	5～10	—	
Run-II	1.90×10^1	7.34	23.0	2.30	—	—	1.30×10^2	2～10	—	I
Run-III	1.90×10^1	11.7	43.3	1.80	—	—	5.31×10^2	2～10	—	

14 cm

Table 1.

	Wind Tunnel Experiment		JONSWAP-observation
	Transition Stage	Stage of Sea-waves	
A_α	14.5	5.47	1.24
P_α	0.375	0.600	0.600
A_β	0.213	0.213	0.675×10^{-3}
P_β	1.00	1.00	1.40

7 cm

Table 2.

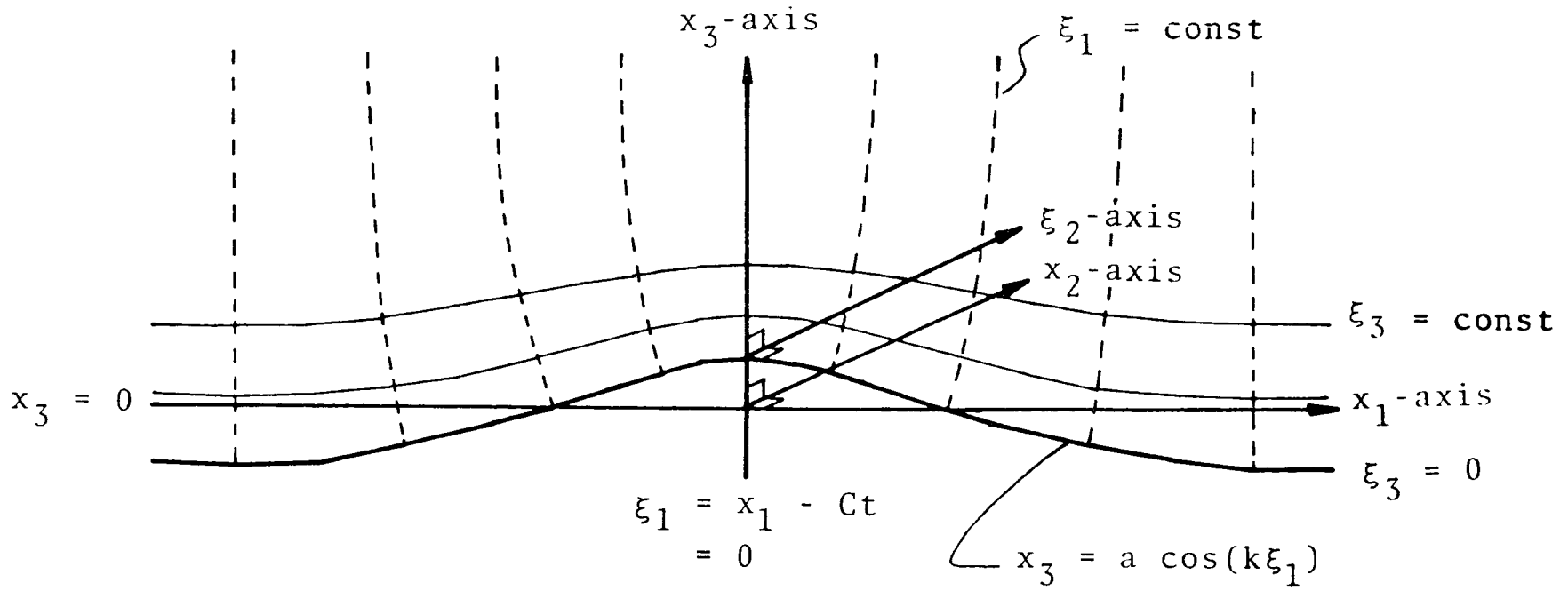
x_3-axis
ξ_1 = const
ξ_2-axis
x_2-axis
ξ_3 = const
x_3 = 0
x_1-axis
ξ_3 = 0
$\xi_1 = x_1 - Ct$
= 0
$x_3 = a \cos(k\xi_1)$

17 cm

Fig. 1.

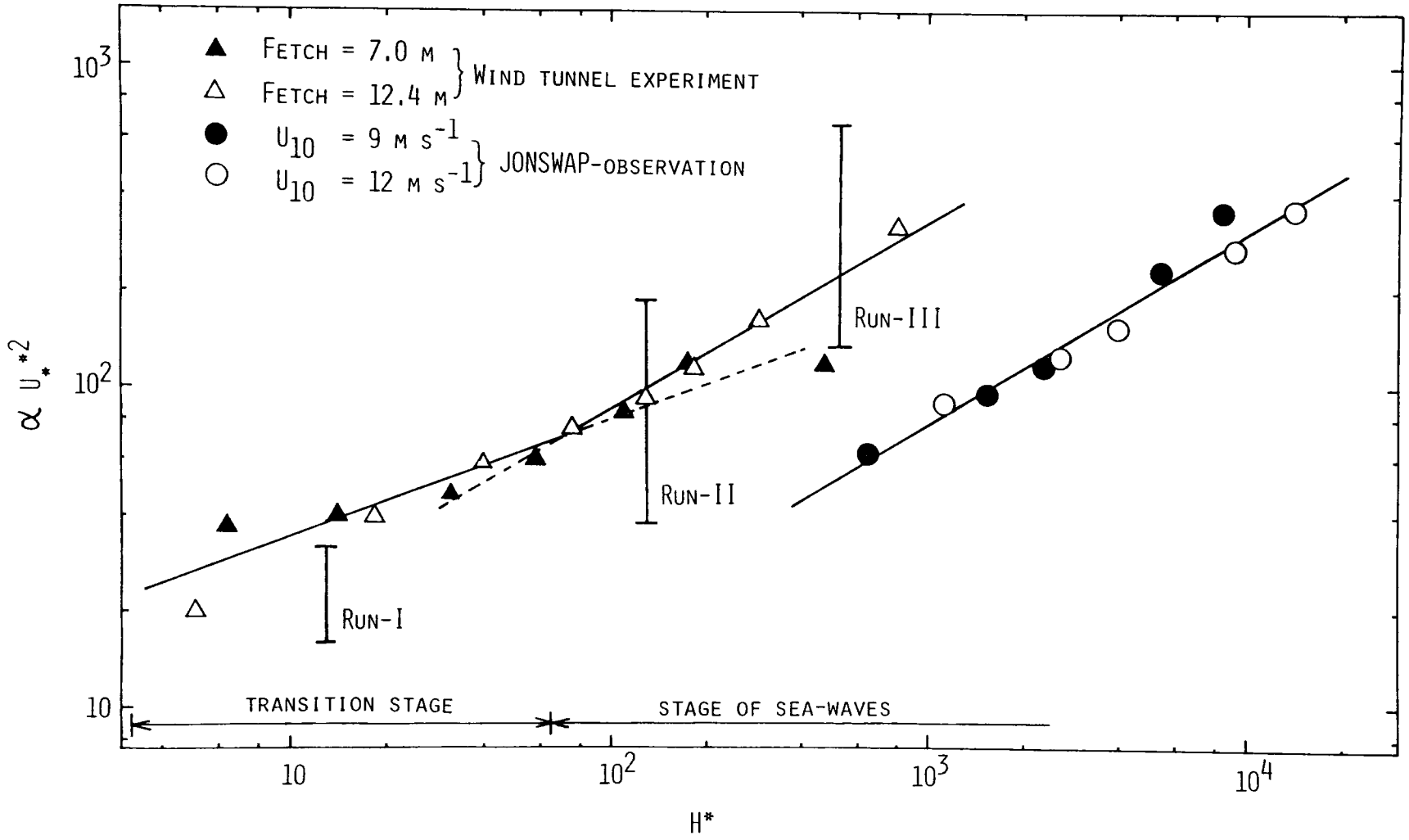
FETCH = 7.0 M
FETCH = 12.4 M
WIND TUNNEL EXPERIMENT
U_{10} = 9 M S^{-1}
U_{10} = 12 M S^{-1}
JONSWAP-OBSERVATION
RUN-I
RUN-II
RUN-III
TRANSITION STAGE
STAGE OF SEA-WAVES
αU_*^2
H_*
10^3
10^2
10
10^4

9cm

Fig. 2.

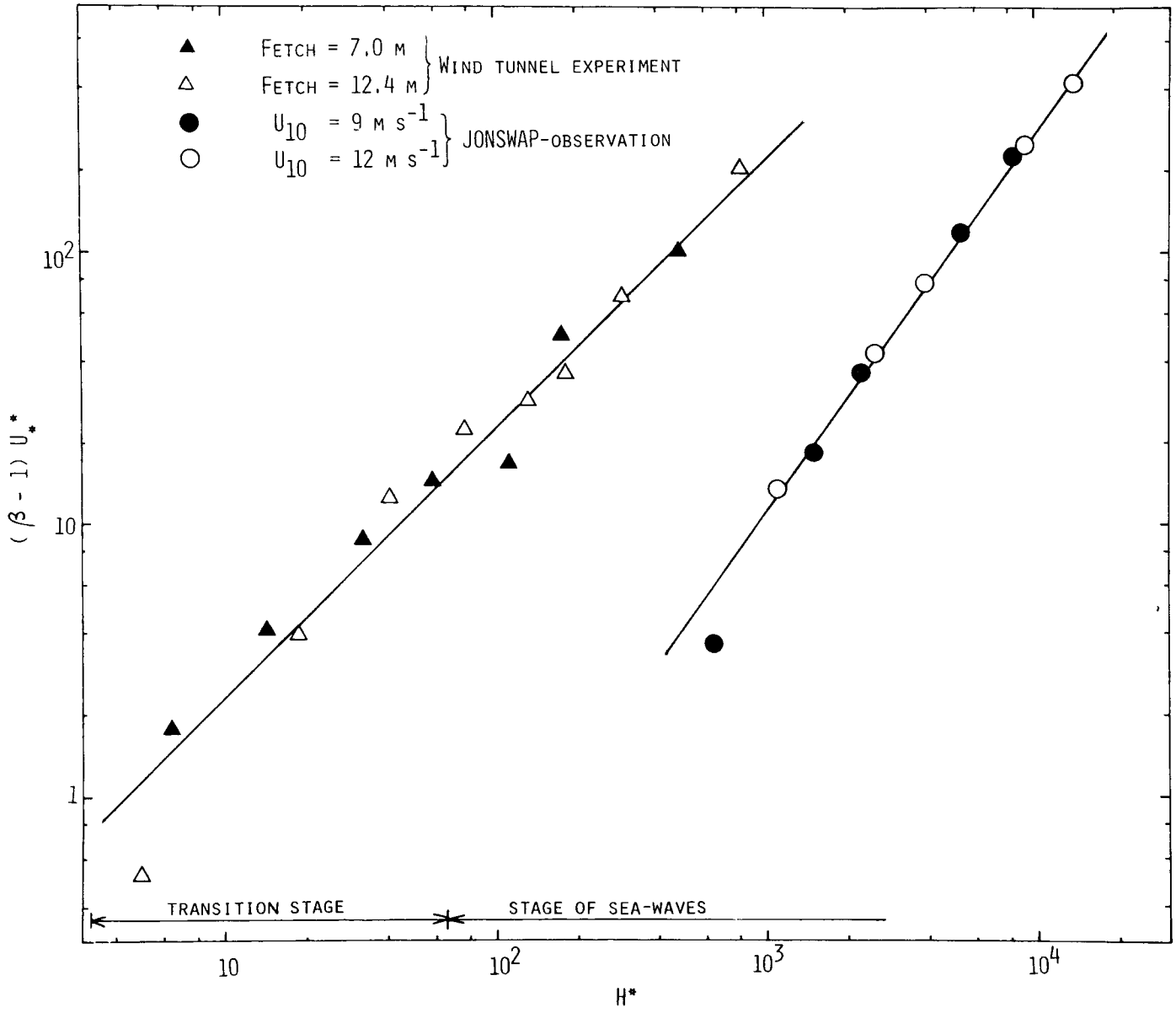
FETCH = 7.0 M
FETCH = 12.4 M
WIND TUNNEL EXPERIMENT
U_{10} = 9 M S^{-1}
U_{10} = 12 M S^{-1}
JONSWAP-OBSERVATION
10^2
10
1
$(\beta - 1)\, U_*^*$
TRANSITION STAGE
STAGE OF SEA-WAVES
10
10^2
10^3
10^4
H*

17 cm

Fig. 3.

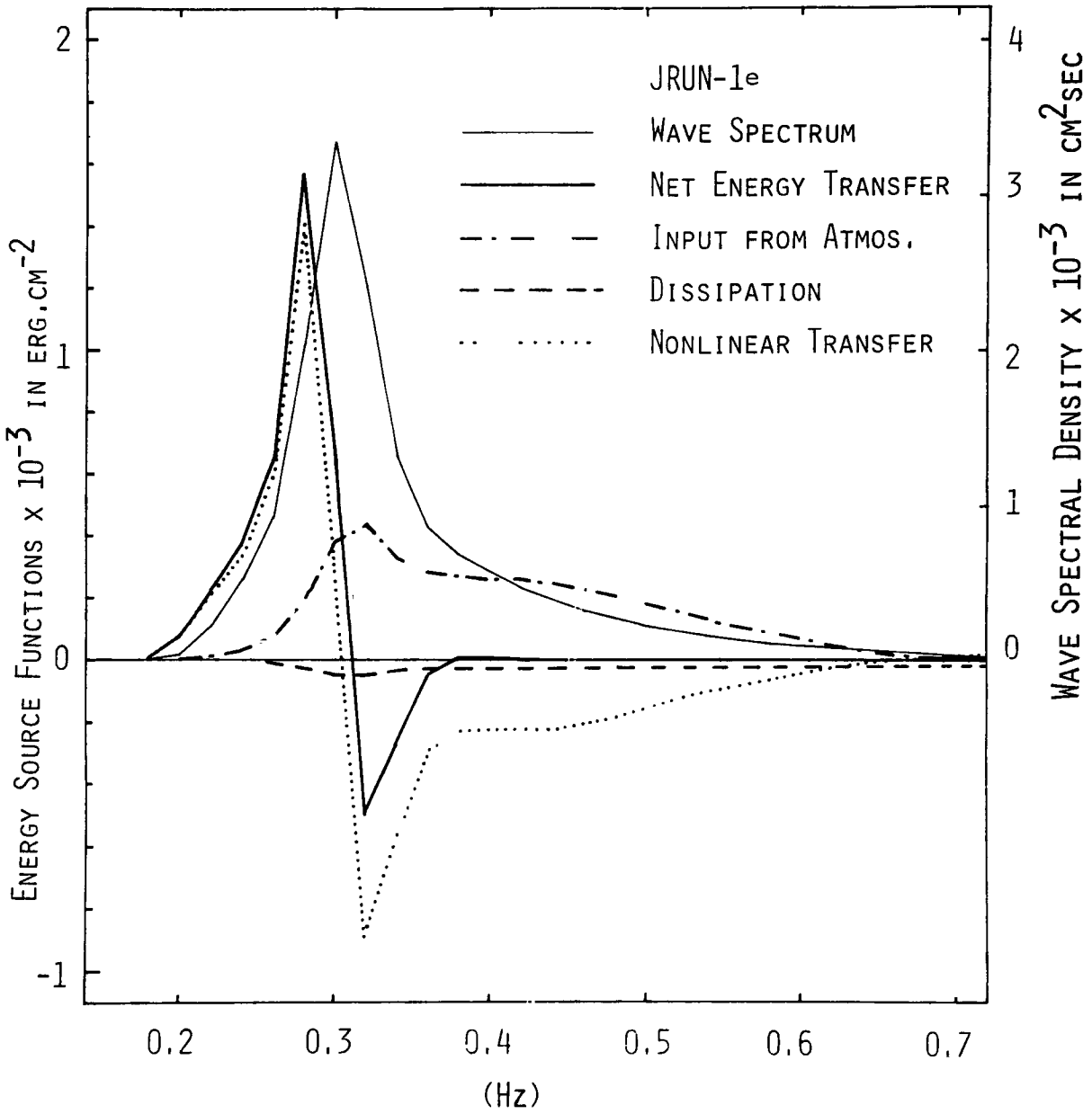
JRUN-1e
WAVE SPECTRUM
NET ENERGY TRANSFER
INPUT FROM ATMOS.
DISSIPATION
NONLINEAR TRANSFER
ENERGY SOURCE FUNCTIONS x 10^-3 IN ERG.CM^-2
WAVE SPECTRAL DENSITY x 10^-3 IN CM^2SEC
2
1
0
-1
4
3
2
1
0
0.2
0.3
0.4
0.5
0.6
0.7
(Hz)

7 cm

Fig. 4.

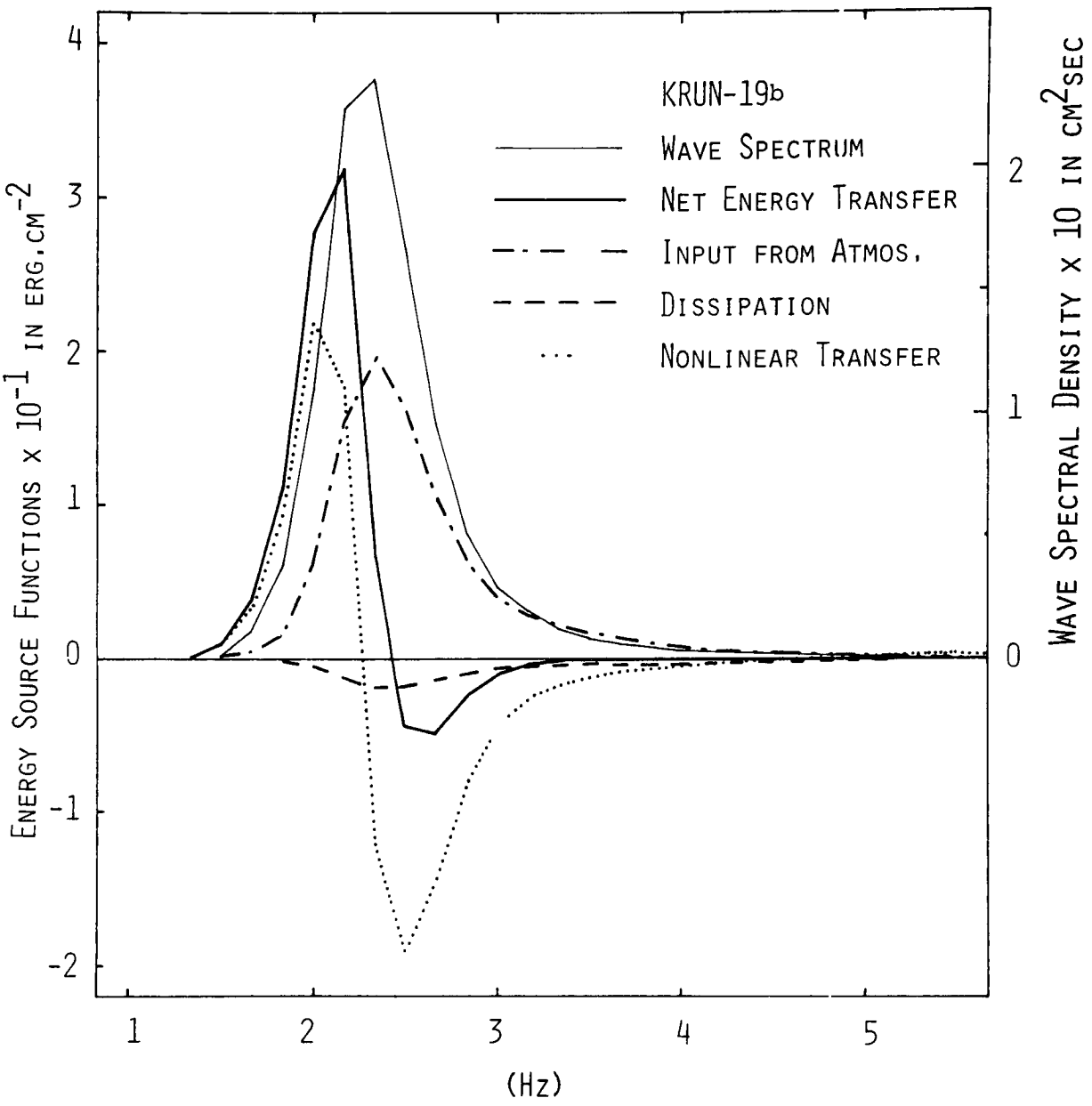
KRUN-19b
WAVE SPECTRUM
NET ENERGY TRANSFER
INPUT FROM ATMOS.
DISSIPATION
NONLINEAR TRANSFER
ENERGY SOURCE FUNCTIONS x 10^-1 IN ERG.CM^-2
WAVE SPECTRAL DENSITY x 10 IN CM^2SEC
(Hz)
4
3
2
1
0
-1
-2
1
2
3
4
5

7cm

Fig. 5.

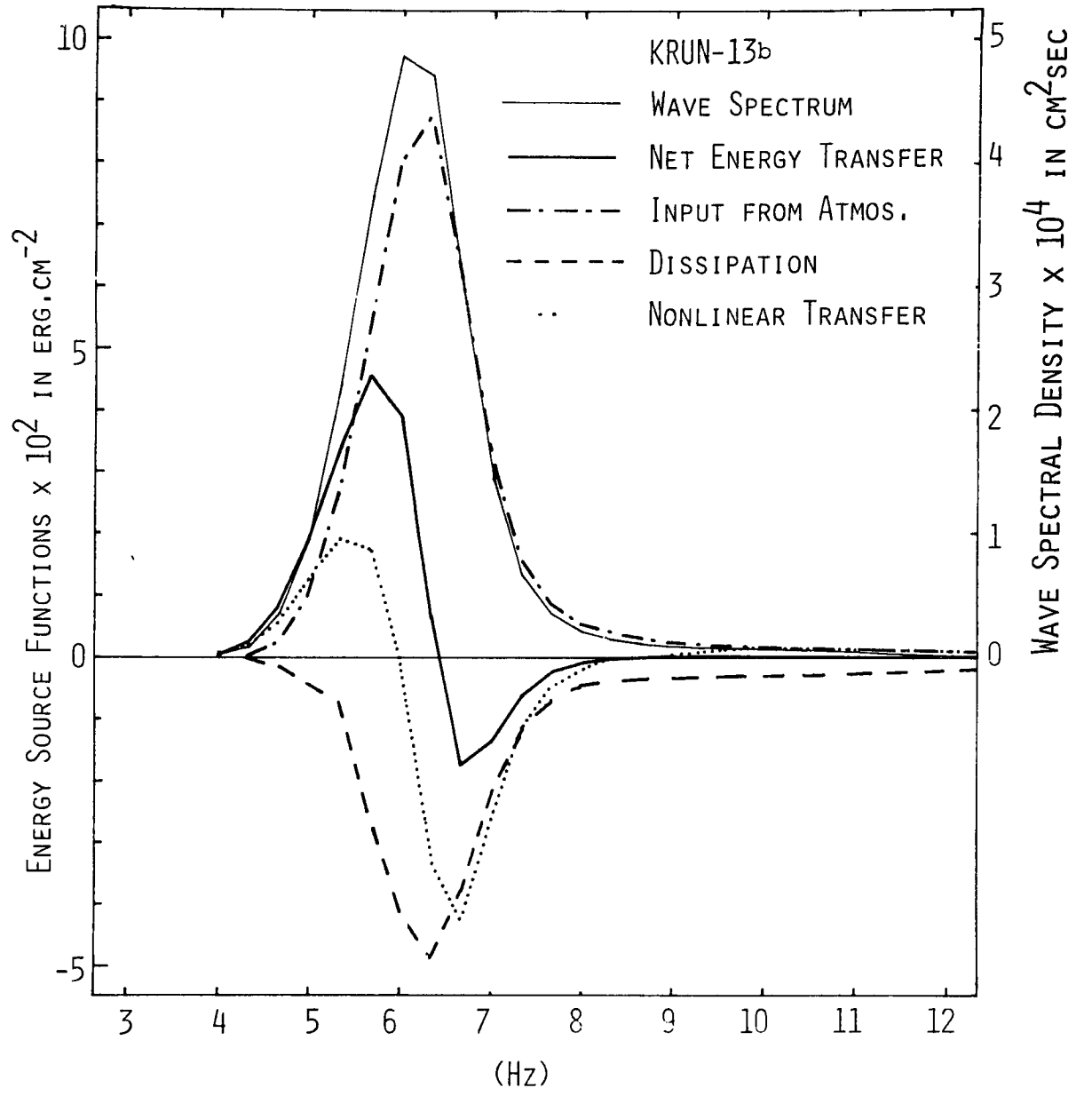
KRUN-13b
WAVE SPECTRUM
NET ENERGY TRANSFER
INPUT FROM ATMOS.
DISSIPATION
NONLINEAR TRANSFER
ENERGY SOURCE FUNCTIONS x 10^2 IN ERG.CM^-2
WAVE SPECTRAL DENSITY x 10^4 IN CM^2SEC
10
5
0
-5
5
4
3
2
1
0
3
4
5
6
7
8
9
10
11
12
(Hz)

7 cm

Fig. 6.

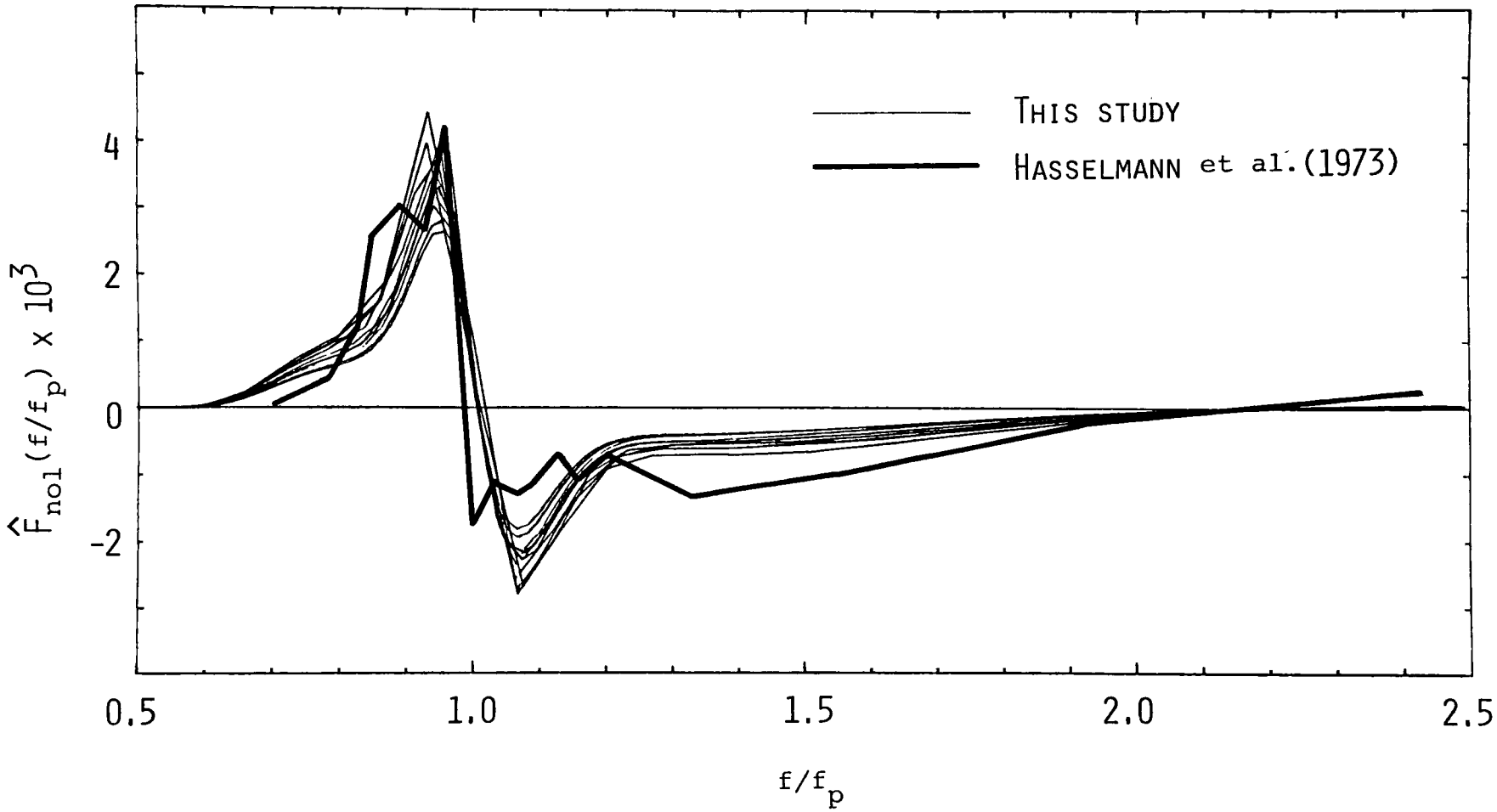
THIS STUDY
HASSELMANN et al.(1973)
$\hat{F}_{nol}(f/f_p) \times 10^3$
4
2
0
-2
0.5
1.0
1.5
2.0
2.5
f/f_p

17 cm

Fig. 7.